
Theses and Dissertations

Fall 2015

Generating analysis-ready NURBS models of cloth for isogeometric analysis

Zhiyu Sun
University of Iowa

Copyright 2015 Zhiyu Sun

This thesis is available at Iowa Research Online: <http://ir.uiowa.edu/etd/2015>

Recommended Citation

Sun, Zhiyu. "Generating analysis-ready NURBS models of cloth for isogeometric analysis." MS (Master of Science) thesis, University of Iowa, 2015.
<http://ir.uiowa.edu/etd/2015>.

Follow this and additional works at: <http://ir.uiowa.edu/etd>



Part of the [Mechanical Engineering Commons](#)

Generating Analysis-Ready NURBS Models of Cloth for Isogeometric Analysis

by

Zhiyu Sun

A thesis submitted in partial fulfillment of the requirements
for the Master of Science degree in Mechanical Engineering
in the Graduate College of The University of Iowa

December 2015

Thesis Supervisor: Professor Jia Lu

Graduate College
The University of Iowa
Iowa City, Iowa

CERTIFICATE OF APPROVAL

MASTER'S THESIS

This is to certify that the Master's thesis of
Zhiyu Sun

has been approved by the Examining Committee
for the thesis requirement for the Master of Science
degree in Mechanical Engineering at the
December 2015 graduation.

Thesis Committee: _____
Jia Lu, Thesis Supervisor

Hiroyuki Sugiyama

Stephen Baek

ABSTRACT

Non-uniform rational basis spline (NURBS) is a geometric language which has been commonly used in computer graphics and Computer Aided Design over years, due to its great flexibility and precision for handling modeled shapes. In computer-aided design, NURBS has become part of industry standards. In most CAD programs every solid model is described by NURBS and stored in NURBS data structure. Recently, the geometric basis function of NURBS is directly used in analysis, leading to the birth of a new area of computational mechanics called isogeometric analysis (IGA). Compared with the traditional finite element analysis, IGA eliminates the disconnection between analysis and design at the geometric level, showing superiority on efficiency and accuracy over the traditional finite element method.

This thesis focuses on the development of an IGA preprocessor for converting an original CAD model (2D-NURBS model) to an ASG (analysis suited geometry) model. ASG means models with mesh quality suitable for analysis. Core technologies utilized during the development include the well-developed NURBS algorithm of knot insertion and knot removal, and a self-developed technology of constructing and utilizing “multi-patch tree”. The developed IGA preprocessor is utilized to process a body armour model consisting of multiple NURBS patches with overly dense meshes. After the processing, the output model has a relatively reasonable elements distribution; the uniformity of the mesh across presumably contact patch boundaries is rebuilt.

PUBLIC ABSTRACT

In garment design field now-a-days, the traditional manual methods of designing and clothing construction have been taken by digital technologies, most designing and clothing construction tasks are completed by utilizing a varies of CAD/CAM programs. With the assistance of CAD software, designer can “sew” cloth patters together, and watch the try-on effect by putting them on a virtual model before actually making a real prototype.

NURBS is de-facto industrial standard for geometric description in most CAD programs. Consequently, the constructed cloth models are always represented by NURBS; 2D NURBS patch models are commonly utilized in cloth modeling. This thesis focuses on the development of an IGA preprocessor for converting an original cloth model (2D-NURBS model) to a model that suits for cloth simulation. Core technologies utilized during the development include the well-developed NURBS algorithm of knot insertion and knot removal, and a self-developed technology of constructing and utilizing “multi-patch tree”. The developed IGA preprocessor is utilized to process a body armour model consisting of multiple NURBS patches with overly dense meshes. After the processing, the output model to some extent becomes an analysis-ready model with some key factors satisfied.

TABLE OF CONTENTS

LIST OF TABLES	vi
LIST OF FIGURES	vii
CHAPTER 1	1
INTRODUCTION	1
1.1 Introduction to Isogeometric Analysis.....	1
1.2 Introduction of IGA Preprocess	2
1.3 Goals of Present Work	4
1.4 Organization of the Thesis	4
CHAPTER 2	6
NURBS BACKGROUND	6
2.1 NURBS ORIGIN	6
2.2 NURBS CURVE.....	8
2.2.1 NURBS curve basics.....	8
2.2.2 NURBS curve segment structure	9
2.2.3 NURBS curve properties	13
2.3 NURBS Surface	14
2.3.1 NURBS surface basics.....	14
2.3.2 NURBS surface element	15
2.3.3 NURBS surface mesh	17
2.4 NURBS Algorithms	19
2.4.1 Knot Insertion	19
2.4.2 Knot Removal	20
2.4.3 Algorithms implementation to NURBS surface	21
CHAPTER 3	23
MULTI-PATCH NURBS SURFACE ADJUSTING PROCESSOR	23
3.1 Data structure construction	23
3.2 Data import and export	25
3.3 Geometric computation.....	26

3.4 Single-patch adjusting.....	28
3.4.1 Elements statistics.....	29
3.4.2 Undersize element elimination	30
3.4.3 Oversize element refinement	31
3.4.4 Disparity over single-patch adjusting	32
3.5 Multi-patch adjusting.....	33
3.5.1 Contact Searching	33
3.5.2 Multi-patch tree construction.....	35
3.5.3 Adjusting process.....	40
3.5.4 Contact boundary modification.....	45
3.5.5 Disparity over Multi-patch adjusting	46
3.6 Originally mis-matched boundaries	47
3.6.1 Searching criteria update.....	49
3.6.2 Knots synchronization over contact patches.....	50
CHAPTER 4	53
APPLICATION ON RAW CAD MODEL	53
4.1 Description of original CAD model.....	53
4.2 Statistics on original mesh of body armour	56
4.3 Individual patch mesh adjusting	60
4.4 Knots Synchronization.....	66
4.5 Multi-patch mesh adjusting.....	71
4.5.1 Elements breaking.....	71
4.5.2 Elements refinement	75
4.6 Conclusions.....	82
CHAPTER 5	83
CONCLUSIONS	83
REFERENCES	84

LIST OF TABLES

Tables:

Table 2.1: NURBS curve segments	10
Table 2.2: NURBS patch elements	16
Table 3.1: Disparities over mesh adjusting of “BELT”	32
Table 3.2: Disparities over multi-patch model adjusting of “VEST”	47
Table 4.1: Summary of patches information on original mesh of body armour	57
Table 4.2: Lower Bound Standard	59
Table 4.3: Updated Patches information with Lower Bound	59
Table 4.4 Summary of patches information on updated mesh of body armour with undersize elements eliminated	65
Table 4.5 Summary of patches information of the updated mesh of body armour after imbalanced elements adjustment	74
Table 4.6 Summary of patches information on final updated mesh of body armour	81

LIST OF FIGURES

Figures:

Figure 2.1: De Boor’s recursive triangle.....	11
Figure 2.2: NURBS basis functions.....	12
Figure 2.3: NURBS curve with segments.....	12
Figure 2.4: Topological mesh.....	18
Figure 3.1: Data structure Basis.....	24
Figure 3.2: Schematic diagram of data import and export structure used in this study.....	25
Figure 3.3: Data flow in structure.....	28
Figure 3.4: Original mesh of Single-patch model “BELT”.....	30
Figure 3.5: Updated mesh of Single-patch model “BELT” with undersize elements eliminated.....	31
Figure 3.6: Adjusting completed mesh of Single-patch model “BELT”.....	32
Figure 3.7: New parameters developed in Data Structure after contact searching.....	35
Figure 3.8: Flow chart of Patch-tree construction.....	38
Figure 3.9: Parameters of NURBS-patch in Data structure with Patch-tree developed.....	39
Figure 3.10: Original mesh of ideal designed (contact boundaries mesh fitted) Multi-patch model “VEST”.....	41
Figure 3.11: Updated mesh of ideal design Multi-patch model “VEST” with undersize elements eliminated.....	43
Figure 3.12: Updated mesh of ideal design Multi-patch model “VEST” with all elements in desired size range.....	44
Figure 3.13: Adjusting completed mesh of ideal designed Multi-patch model “VEST” with modified contact boundaries.....	46

Figure 3.14: Original mesh of raw designed (contact boundaries mesh not fitted) Multi-patch model “VEST”	48
Figure 3.15: New parameter of NURBS-curve developed for updated searching criteria.....	50
Figure 3.16: Updated mesh of raw designed Multi-patch model “VEST” with knots synchronized over contact patches.....	51
Figure 3.17: Adjusting completed mesh of raw designed Multi-patch model “VEST”	52
Figure 4.1: Front vision of original mesh of body armour	54
Figure 4.2: Perspective vision of original mesh of body armour.....	55
Figure 4.3: Sleeve zoom in of original mesh of body armour	56
Figure 4.4: Front vision of updated mesh of body armour with undersize elements eliminated	62
Figure 4.5: Perspective vision of updated mesh of body armour with undersize elements eliminated	63
Figure 4.6: Trouser zoom in of updated mesh of body armour with undersize elements eliminated	64
Figure 4.7: Front vision of updated mesh of body armour with knots synchronized	68
Figure 4.8: Perspective vision of updated mesh of body armour with knots synchronized	69
Figure 4.9: Trouser part zoom in of updated mesh of body armour with knots synchronized	70
Figure 4.10: Front vision of updated mesh of body armour after imbalanced elements adjusted	72
Figure 4.11: Perspective vision of updated mesh of body armour after imbalanced elements adjusted.....	73
Figure 4.12: Front vision of final updated mesh of body armour.....	76

Figure 4.13: Perspective vision of final updated mesh of body armour	77
Figure 4.14: Sleeve zoom in of final updated mesh of body armour.....	78
Figure 4.15: Trouser zoom in of final updated mesh of body armour	79
Figure 4.16: Trouser part zoom in of final updated mesh of body armour.....	80

CHAPTER 1

INTRODUCTION

1.1 Introduction to Isogeometric Analysis

Isogeometric analysis is a new development in computational mechanics. The essential idea of IGA is to use the same geometric language in Computer Aided Design (CAD) and analysis [1]. This approach is an advancement of finite element method. Finite element method essentially uses Lagrangian polynomials to construct assumed solutions, while the geometric basis function used in CAD is different. Therefore, a disconnection between finite element analysis and design is unavoidable, and this has been the root cause of many practical issues arising in computer aided engineering. In finite element method, a mesh must be generated to approximate the original CAD geometry before analysis. Approximating the geometry using mesh is a source of modeling error. The construction of finite element geometry, including meshing and mesh manipulation, can be very costly and time consuming. The goal of IGA is to tightly connect design with analysis by using the same geometric basis functions, and eliminating the need for communication with the CAD geometry [1, 20, 21].

Presently, NURBS (Non-Uniform Rational B-Splines) is the most widely used geometric language in isogeometric analysis. NURBS has become the de-facto industrial standard for geometric description, design, and graphic data exchange in most CAD programs. Industrial standards such as IGES, STEP, and PHIGS, all recognize NURBS for geometric design [3]. With a unified mathematical basis, NURBS has good performance in representing both analytic shapes and free-form entities. Conic sections and quadric

surfaces can be accurately represented by NURBS. While utilized in analysis, the NURBS geometry can maintain higher levels of continuity across element boundaries. Due to its excellent properties and enormous popularity in the CAD world, NURBS plays a leading role in the area of IGA.

T-splines is a variant of NURBS with increasing popularity in the last few years. It has the advantage of local refinement and coarsening, compared with NURBS. In addition, it can significantly reduce the computational expense when sewing together adjacent patches [4, 5].

1.2 Introduction of IGA Preprocess

The concept of isogeometric analysis, first introduced by Hughes et al., was initially motivated by the need of integrating Computer Aided Design (CAD) and finite element analysis (FEA)[1]. When generating a FEM mesh from a CAD models, firstly, geometric ambiguities such as gaps and overlaps in the model must be removed, to arrive at an Analysis Suitable Geometry [6]. This ASG is then replaced with a finite element mesh. Frequently, obtaining an accurate FEM solution needs a series of refinements which often requires mesh adaptation or regeneration [7]. During mesh refinement, a link must be established between the ASG and the refinement routine [4]. Thus, prior to analysis and during adaptive steps, a large amount of effort is spent on mesh manipulation [8]. In IGA, the idea is to have only one representation of the geometry which exactly describes the ASG, and one that is more faithful to the initial CAD model. There is then no need for reestablishing an external description of the geometry. Although in IGA the issues of the generation and refinement of the external mesh do not exist anymore, there is still the need to obtain a good quality ASG. Once the ASG is constructed, the meshes are intrinsically

defined by the NURBS data structure [9]. The quality of the ASG is then critically important in ensuring mesh quality. A few researchers have been addressed this issue [7, 10-13]. The concept of “analysis-aware geometry modeling” was proposed by the authors in [7]. The process of deriving a good quality ASG from an initial CAD model not suited for analysis can be defined as IGA preprocess.

In garment industry now-a-days, virtual prototyping has become popular [22, 31]. With the assistance of CAD software, designer can “sew” cloth patters together, and watch the try-on effect by putting them on a virtual model before actually making a real prototype. Garment CAD methods have revolutionized the garment designed business, most designing and clothing construction tasks are completed by utilizing varies of CAD/CAM programs [23]. Some typical commercial softwares of garment CAD include Gerber in United States [24], Investronica in Spain [25], Lectra in France [26], Assyst-Bullmer in German [27] and Dessingsim in Japan [28]. As we know, NURBS is de-facto industrial standard for geometric description in most CAD programs. Consequently, the constructed cloth models are always represented by NURBS; 2D NURBS patch models are commonly utilized in cloth modeling. As cloth can be consider as thin fabrics (the thickness h is less than $1/20$ of the characteristic length in the lateral direction), it can be effectively described by Kirchhoff–Love shell theory [14]. Due to the maintainability of a C^1 or higher order continuities, NURBS geometry naturally supports the Kirchhoff–Love analysis. With some advantages in comparison to the Reissner–Mindlin formulation in finite element geometry [30, 31], NURBS Kirchhoff–Love element is developed to be utilized in IGA for cloth simulation [15]. However most original CAD model of cloth does not suit for directly applying the IGA due to the initial mesh quality. A development of the IGA preprocessor

for generating analysis-ready NURBS models for cloth is motivated by solving such issue. Although the scope of the preprocessor application is particular on cloth modeling, the method in principle has the capability to apply to all 2D NURBS problem.

1.3 Goals of Present Work

The goal of this thesis is to develop an IGA preprocessor for converting a 2D CAD model to an ASG model. The particular application of the study is cloth modeling. In our IGA preprocessor, the desired quality of mesh are evaluated by two aspects: (1) a relatively uniform distribution of elements in a desired element size range for each sub-region NURBS surface; (2) compatibility of mesh across common boundary edges in Multi-patch NURBS model.

To develop a preprocessor for cloth modeling or generally 2D application, the following tasks are pursued: (1) constructing a data structure to store all essential parameters of a CAD model; (2) utilizing the knot insertion and removal algorithm to achieve mesh adjusting goals for single-patch model; (3) constructing “multi-patch tree” to extend the mesh adjusting process to multi-patch model; (4) developing the technologies to make the mesh adjusting process capable to handle real world models with mismatched descriptions for presumably contact boundaries.

1.4 Organization of the Thesis

The thesis is organized as follows. Chapter 2 introduces the background of NURBS, including its origin, basis, geometric express and geometric algorithm, etc. Chapter 3 describes the IGA preprocessor developed in this work, and demonstrates how it works.

An application of the IGA preprocessor to armor models is presented in Chapter 4. Some conclusions and limitations of the work are presented in Chapter 5.

CHAPTER 2 NURBS BACKGROUND

Non-Uniform Rational B-Splines, commonly referred to as NURBS, is derived from the Bezier curve discovered by Pierre Bezier in the late 1960's and early 1970's.[16] Due to the excellent mathematical and algorithmic properties, NURBS is now well established in curve and surface representation and has become an industry standard for the geometric representation and data exchange of geometric information in the CAD/CAM/CAE world.[3]

2.1 NURBS ORIGIN

CAD geometry starts from Bezier curves. A Bezier curve is a parametric polynomial curve using the Bernstein polynomials as basis. An n th-degree Bezier curve is defined by

$$\mathbf{C}(u) = \sum_{i=0}^n B_{i,n}(u)\mathbf{P}_i \quad 0 \leq u \leq 1 \quad (2.1)$$

where $B_{i,n}(u)$ are the n th-degree Bernstein polynomials described by

$$B_{n,i}(u) = \frac{n!}{i!(n-i)!} u^i (1-u)^{n-i}, \quad 0 \leq u \leq 1 \quad (2.2)$$

$\{\mathbf{P}_i\}$ are called control points which act as the geometric coefficients of this form. Notable properties of Bezier curves are showed as follows: (1) the curve passes through the end points \mathbf{P}_0 and \mathbf{P}_n , the so-called endpoint interpolation property; (2) the curve can be translated, rotated, stretched and sheared simply by applying the transformation to the control points; (3) the curve can be split at any point into two sub-curves, or into arbitrarily many sub-curves, each one of them is also a Bezier curve.

Bezier curves still have some shortcomings. First and foremost, a Bezier curve is a single polynomial segment. To describe a complex curve with a single polynomial, the degree of the polynomial must be high enough, and a large number of constraints needs to be satisfied. Also single-segment curves are not suited to interactive shape design [3], because change any of its parameters would change the object globally. These issues were addressed by B-splines [16].

B-splines are piecewise Bezier curves with same polynomial degree and a controllable degree of continuity at joints. A p th-degree B-spline curve is described by

$$\mathbf{C}(u) = \sum_{i=0}^n N_{i,p}(u) \mathbf{P}_i \quad a \leq u \leq b \quad (2.3)$$

$\{\mathbf{P}_i\}$ are still control points, and $N_{i,p}(u)$ are the normalized B-spline basis functions. There are many ways to define the B-splines basis functions, here we follow the Cox-de Boor recursion formula [3], due to its convenience for computer implementation.

A knot vector is a non-decreasing sequences of real numbers in the form of $U = \{u_0, \dots, u_m\}$ i.e., $u_i \leq u_{i+1}$ $i = 0, \dots, m - 1$. The knot vector defines the parametric space of a B-spline curve. The i th B-spline basis function of p -degree is defined as

$$N_{i,p}(u) = \begin{cases} 1, & u_i \leq u < u_{i+1} \\ 0, & \text{otherwise} \end{cases}$$

$$N_{i,p}(u) = \frac{(u - u_i)}{(u_{i+p} - u_i)} N_{i,p-1}(u) + \frac{(u_{i+p+1} - u)}{(u_{i+p+1} - u_{i+1})} N_{i+1,p-1}(u) \quad (2.4)$$

NURBS are rational B-splines. Rational curves originate from projective geometry. A NURBS curve in d -dimensional Euclidean space is the projection of a B-spline curve of

dimension $d+1$. The “coordinates” in the additional dimension are called weights. A p th-degree NURBS curve is described by

$$\mathbf{C}(u) = \frac{\sum_{i=0}^n N_{i,p}(u)w_i \mathbf{P}_i}{\sum_{i=0}^n N_{i,p}(u)w_i} \quad a \leq u \leq b \quad (2.5)$$

The NURBS database contains four sets of control parameters: (1) control points (\mathbf{P}_i); (2) knot vector (knot: u); (3) degree (p) and (4) weights (w_i). The first three are the same as the B-spline curve described above. The B-spline basis function $N_{i,p}(u)$ can be completely determined by the knot vector and degree. The weights are additional parameters demonstrating the projection from projective geometry. Emphasizing the physical coordinates, a NUBRS curve is usually represented by

$$\mathbf{C}(u) = \sum_{i=0}^n R_{i,p}(u) \mathbf{P}_i ; R_{i,p}(u) = \frac{N_{i,p}(u)w_i}{\sum_{i=1}^n N_{i,p}(u)w_i} \quad (2.6)$$

$R_{i,p}(u)$ represents the i th NURBS basis function of p -degree.

2.2 NURBS CURVE

2.2.1 NURBS curve basics

A NURBS curve is determined by control parameters, including control points, knot vector, degree and weights. In a p th-degree NURBS curve with u in an interval $[a, b]$ (defined as formula 2.5), if the first and the last knot each repeats $p+1$ times, namely = $\{\underbrace{a, \dots, a}_{p+1}, u_{p+2}, \dots, u_{m-p-1}, \underbrace{b, \dots, b}_{p+1}\}$, the curve passes the first and the last control points.

Any interior knot can be repeated up to p times. Each time a knot is repeated once, the continuity at that location will be decreased by one. The number of knots (counting

multiplicity), m , the number of control points, n , knots, m and the degree, p , satisfy the relation, as described by the following equation:

$$m = n + p + 1 \quad (2.7)$$

The weights are associated with the control points one by one with a total number of n . The number of B-spline basis functions ($N_{i,p}(u)$) or NURBS basis functions ($R_{i,p}(u)$) is n .

2.2.2 NURBS curve segment structure

B-splines are piecewise polynomials. A B-spline curve is a composition of Bezier segments. Accordingly, a NURBS curve is also a composition of rational Bezier segments. Each individual segment of a NURBS curve is completely specified by a local knot vector and a subset of control points with the corresponding weights. In isogeometric analysis, each segment naturally becomes an element [17, 18].

An example is presented to demonstrate the segment structure of a NURBS curve. A NURBS curve in two dimension space is created with the knot vector $U = \{0, 0, 0, 1, 2, 3, 3, 3\}$, the degree $p = 2$ and the control points and weights showing bellow.

$$\begin{aligned} P &= \{P_0, P_1, P_2, P_3, P_4\} \\ &= \{\{0,0\}, \{1,2\}, \{2.5,0\}, \{4,2\}, \{5,0\}\} \end{aligned}$$

$$W = \{W_0, W_1, W_2, W_3, W_4\} = \{1,1,1,1,1\}$$

The NURBS curve is composed of 3 segments, and the breakout is shown in following table.

Table 2.1: NURBS curve segments

Segment	Knot Interval	Local Knot Vector	Segment Related Basis	Control Points	Weights
1	[0,1]	{0,0,0,1,2,3}	$R_{0,2}, R_{1,2}, R_{2,2}$	P_0, P_1, P_2	W_0, W_1, W_2
2	[1,2]	{0,0,1,2,3,3}	$R_{1,2}, R_{2,2}, R_{3,2}$	P_1, P_2, P_3	W_1, W_2, W_3
3	[2,3]	{0,1,2,3,3,3}	$R_{2,2}, R_{3,2}, R_{4,2}$	P_2, P_3, P_4	W_2, W_3, W_4

For each segment, the corresponding NURBS basis functions can be completely determined by the local knot vector. De Boor's recursive triangle, as shown in Figure 2.1, demonstrates such procedure. Each segment is controlled by local control points and weights that have influence on this segment. The shape function over entire knot space is shown in Figure 2.2. The entire NURBS curve with three segments marked in different colors is shown in Figure 2.3. Each segment is controlled by three control points. In general, a p th degree NURBS curve segment of a knot interval of $[i, i + 1]$ has a number of $p+1$ corresponding control points, $\{P_i, P_{i+1}, \dots, P_{i+p}\}$.

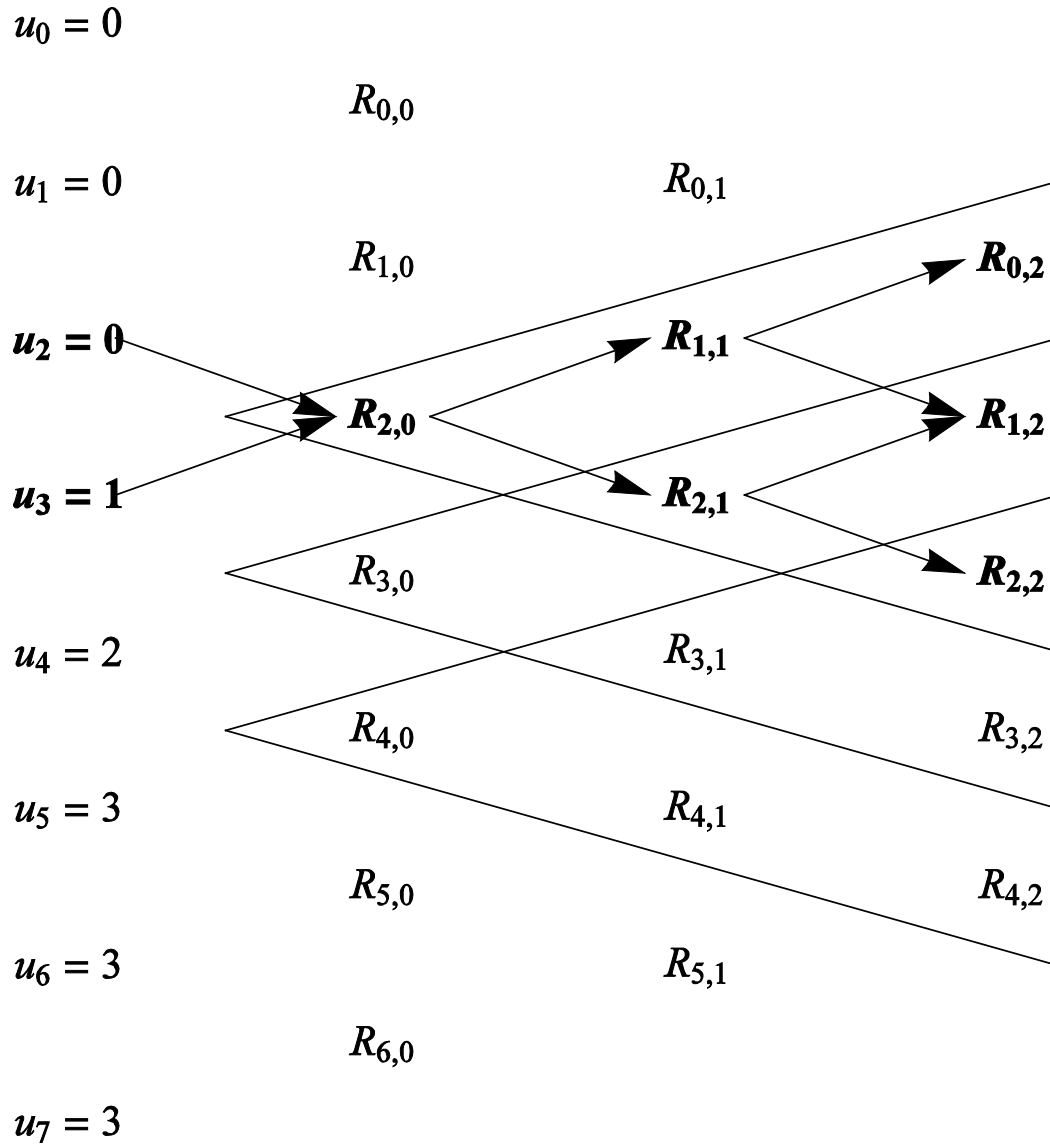


Figure 2.1: De Boor's recursive triangle

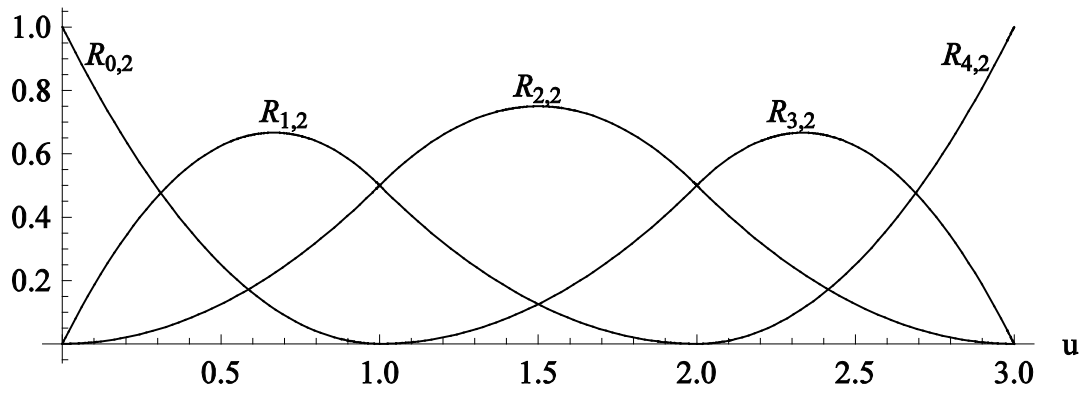


Figure 2.2: NURBS basis functions

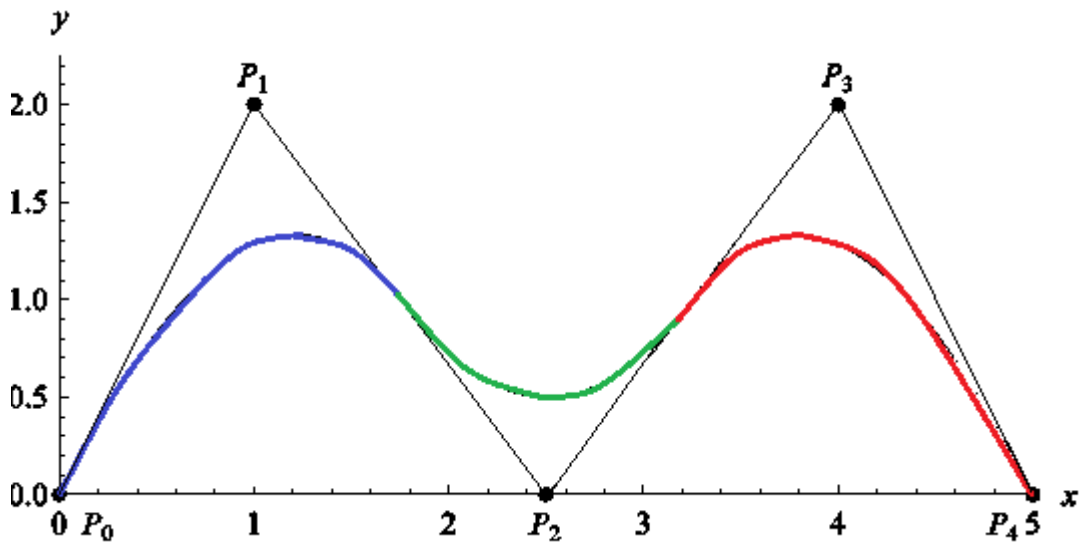


Figure 2.3: NURBS curve with segments

2.2.3 NURBS curve properties

The NURBS curve has the following analytic and geometric properties[3]:

1. Partition of unity: $\sum_{i=0}^n R_{i,p}(u) = 1$
2. Positiveness: if all weights are positive, then $R_{i,p}(u) \geq 0$ for all parameter values.
3. Endpoint interpolation: A NURBS curve passes through its end control points \mathbf{P}_0 and \mathbf{P}_n .
4. Affine invariance: the curve is invariant with respect to affine. Any projective transformation is applied to a NURBS curve by applying it to the control points. This means we can translate, rotate, and stretch and shear the curve simply by applying the transformation to the control points.
5. Local support: the i th basis function is zero outside the interval $[u_i, u_{i+p+1}]$. For any knot span, there are at most $p + 1$ basis functions that are nonzero. This means that changing a control point only affects the curve locally.
6. Smoothness: inside each knot span, the curve is infinitely differentiable. At each knot, if a knot has multiplicity s , the curve is at least $p - s$ times continuously differentiable. If all interior knots are not repeated, the curve is C^{p-1} continuous.

2.3 NURBS Surface

2.3.1 NURBS surface basics

A NURBS surface is generated by taking the tensor product of two NURBS curves in two different directions. A NURBS surface of degree p in the u direction and degree q in the v direction is a bivariate piecewise rational function represented by [3]

$$\mathbf{S}(u, v) = \frac{\sum_{i=0}^n \sum_{j=0}^m N_{i,p}(u) N_{j,q}(v) w_{i,j} \mathbf{P}_{i,j}}{\sum_{i=0}^n \sum_{j=0}^m N_{i,p}(u) N_{j,q}(v) w_{i,j}} \quad (2.8)$$

$$a \leq u \leq b, c \leq v \leq d$$

The $\{\mathbf{P}_{i,j}\}$ form a control bidirectional points net. $\{w_{i,j}\}$ are the weights. $N_{i,p}(u)$ and $N_{j,q}(v)$ are the nonrational B-spline basis functions defined on the two knot vectors with $U = \{\underbrace{a, \dots, a}_{p+1}, u_{p+2}, \dots, u_{r-p-1}, \underbrace{b, \dots, b}_{p+1}\}$ and $V = \{\underbrace{c, \dots, c}_{q+1}, v_{q+2}, \dots, v_{s-q-1}, \underbrace{d, \dots, d}_{q+1}\}$. The number of knots (counting multiplicity) in the knot vector U and V are r and s respectively. n and m are the number of control points along u and v directions, respectively. Following relations exit:

$$\begin{aligned} r &= n + p + 1 \\ s &= m + q + 1 \end{aligned} \quad (2.9)$$

The total number of control points is determined by $n \times m$. The weights are assigned to each control point.

The NURBS surface rational basis function is represented by

$$R_{i,j}(u, v) = \frac{N_{i,p}(u)N_{j,q}(v)w_{i,j}}{\sum_{i=0}^n \sum_{j=0}^m N_{i,p}(u)N_{j,q}(v)w_{i,j}} \quad (2.10)$$

Then formula 2.8 can be written as

$$\begin{aligned} \mathbf{S}(u, v) &= \sum_{i=0}^n \sum_{j=0}^m R_{i,j}(u, v) \mathbf{P}_{i,j} \\ a \leq u \leq b, c \leq v \leq d \end{aligned} \quad (2.11)$$

2.3.2 NURBS surface element

Similar to NURBS curve segment structure introduced in section 2.2.2, a NURBS patch (NURBS surface) is comprised of Bezier elements. Each element is a non-empty tensor product span of the form $[u_k, u_{k+1}] \times [v_l, v_{l+1}]$ in the parametric domain. NURBS surface element is defined exclusively by a set of local parameters as followings.

$$\begin{aligned} U_e &= \{u_{k-p}, \dots, u_k, u_{k+1}, \dots, u_{k+p+1}\} \\ V_e &= \{v_{l-q}, \dots, v_l, v_{l+1}, \dots, v_{l+q+1}\} \\ \{\mathbf{P}_{ij}\}, & \quad j = k - p, \dots, k, \quad j = l - q, \dots, q \\ \{w_{ij}\}, & \quad j = k - p, \dots, k, \quad j = l - q, \dots, q \end{aligned} \quad (2.12)$$

In finite element analysis, all computations are element-centered. The stiffness matrix, residual vectors and all post-processes are computed element-wise. With the above element breakout, the computational structure of FEM can be easily carried over to NURBS isogeometric analysis. Therefore, in IGA the mesh is inherently generated by the segmental structure of the NURBS geometry.

An example is presented here to demonstrate the NURBS element structure in detail. Consider a NURBS patch having the following knot vectors and degrees.

$$U = \{0, 0, 0, 1, 2, 2, 2\}$$

$$V = \{0, 0, 0, 2, 4, 4, 4\}$$

$$p = 2$$

$$q = 2$$

The total number of controls points should be 16 (4×4) and the same for weights. The patch consists of 4 elements with details shown in Table 2.2.

Table 2.2: NURBS patch elements

Elements	Knot span	Element knots	Control Points	Weights
1	$[0,1] \times [0,2]$	$\{0,0,0,1,2,2\}$ $\{0,0,0,2,4,4\}$	P_{11}, P_{12}, P_{13} P_{21}, P_{22}, P_{23} P_{31}, P_{32}, P_{33}	w_{11}, w_{12}, w_{13} w_{21}, w_{22}, w_{23} w_{31}, w_{32}, w_{33}
2	$[1,2] \times [0,2]$	$\{0,0,1,2,2,2\}$ $\{0,0,0,2,4,4\}$	P_{12}, P_{13}, P_{14} P_{22}, P_{23}, P_{24} P_{32}, P_{33}, P_{34}	w_{12}, w_{13}, w_{14} w_{22}, w_{23}, w_{24} w_{32}, w_{33}, w_{34}
3	$[0,1] \times [2,4]$	$\{0,0,0,1,2,2\}$ $\{0,0,2,4,4,4\}$	P_{21}, P_{22}, P_{23} P_{31}, P_{32}, P_{33} P_{41}, P_{42}, P_{43}	w_{21}, w_{22}, w_{23} w_{31}, w_{32}, w_{33} w_{41}, w_{42}, w_{43}
4	$[1,2] \times [2,4]$	$\{0,0,1,2,2,2\}$ $\{0,0,2,4,4,4\}$	P_{22}, P_{23}, P_{24} P_{32}, P_{33}, P_{34} P_{42}, P_{43}, P_{44}	w_{22}, w_{23}, w_{24} w_{32}, w_{33}, w_{34} w_{42}, w_{43}, w_{44}

2.3.3 NURBS surface mesh

Based on the characters of NURBS surface elements, the concept of NURBS mesh is brought out. The topology structure of the NURBS mesh is described by an index mesh and an element mesh.

The index mesh is a rectangular grid in which each line corresponds to a knot index. For the general representation of a NURBS surface, as described in section 2.3.1, there are r and s knots in the U and V knot vectors. The index mesh of a NURBS surface is a $r \times s$ grid, with each horizontal line corresponding to an index of the u -knot and vertical lines for v -knots. The element mesh is a sub-grid which represents all the NURBS elements located in the index mesh. An element corresponding to the non-empty knot span $[u_i, u_{i+1}] \times [v_j, v_{j+1}]$ is represented by the region bounded by horizontal lines $i, i + 1$ and vertical lines $j, j + 1$ in the index mesh. The control point array shows the total number of control points required for a NURBS surface and how they are distributed among elements. The control points of a $p \times q$ degree NURBS element are reflected as a sub-array centered at this element on the index mesh.

An example is presented here to demonstrate the topology structure of NURBS surface mesh more specifically. Consider a NURBS patch having the following knot vectors and degrees.

$$U = \{0, 0, 0, 1, 2, 3, 3, 3\}$$

$$V = \{0, 0, 0, 2, 4, 4, 4\}$$

$$p = 2$$

$$q = 2$$

The index mesh of this NURBS-patch is a 8×7 grid. There are 6 elements in the patch, the element mesh is a 3×2 grid placed in the center of the index mesh. The control points form an 5×4 array with each element bounded by 9 control points. The superposed topological mesh of the NURBS patch is shown in Figure 2.4 (index mesh in black, element mesh in red, and control points array with blue dots).

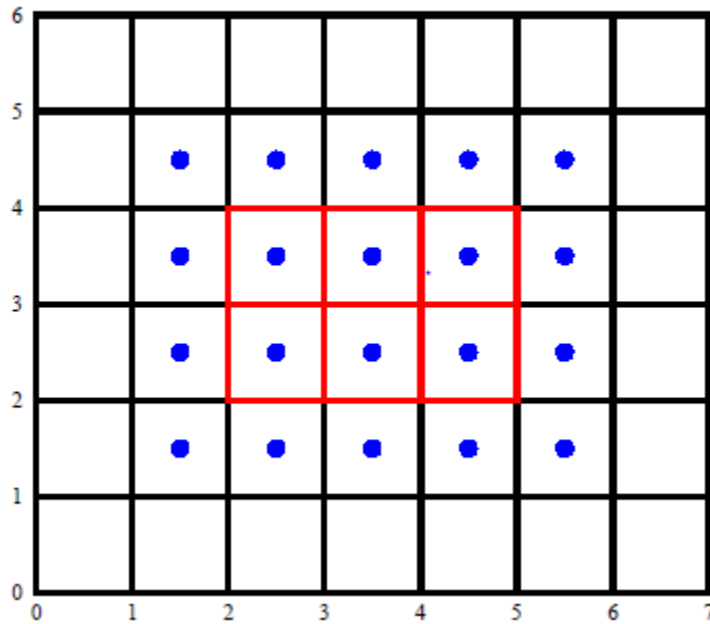


Figure 2.4: Topological mesh

2.4 NURBS Algorithms

Several fundamental geometric algorithms have been developed for NURBS, including knot insertion, knot refinement, knot removal, degree elevation and degree reduction. The core technologies utilized in our IGA preprocessor development include the knot insertion algorithm and the knot removal algorithm. In this section these two algorithms are introduced in detail.

2.4.1 Knot Insertion

Consider a p th degree NURBS curve defined on knot vector $U = (u_1, \dots, u_m)$, control points $P = (P_1, \dots, P_n)$, weights $w = (w_1, \dots, w_n)$. Control points and weights can be combined to an extended parameters $P_i^w = (w_i P_i, w_i)$. Let $\bar{u} \in [u_k, u_{k+1})$, insert \bar{u} into U to form the new knot vector $\bar{U} = (u_1, \dots, u_k, \bar{u}, u_{k+1}, \dots, u_m)$. An insertion in the knot interval $[u_k, u_{k+1})$ will only affect the basis functions that are nonzero in that interval and the corresponding control points. The number of control points will be increased by one. The new control points set is represented by $Q = (Q_1, \dots, Q_{n+1})$. The new control points and weights can be derived from the original ones with following formulas [3].

$$Q_i^w = P_i^w, \quad i = 1, \dots, k - p \quad (2.12)$$

$$Q_{i+1}^w = P_i^w, \quad i = k, \dots, n \quad (2.13)$$

For $i = k - p + 1, \dots, k$

$$Q_i^w = \alpha_i P_i^w + (1 - \alpha_i) P_{i-1}^w, \quad \alpha_i = \frac{\bar{u} - u_{i+1}}{u_{i+p+1} - u_{i+1}} \quad (2.14)$$

Then, a new NURBS curve defined with the new knot vector, control points, and weights is generated. The geometry of the new NURBS curve after the knot insertion is exactly the same as the original one. This is in sharp contrast with finite element mesh refinement. Due to such geometry preservation property, the knot insertion algorithm is a very useful tool for NURBS mesh refinement without changing the original shape of the object.

2.4.2 Knot Removal

For a p th degree NURBS curve defined on knot vector $U = (u_1, \dots, u_m)$, control points $P = (P_1, \dots, P_n)$, weights $w = (w_1, \dots, w_n)$. A removal of a knot u_r from the knot vector U forms the new knot vector $(u_1, \dots, u_{r-1}, u_{r+1}, \dots, u_m)$. As the boundary knots cannot be removed, we have $p + 1 < r < m - p$. The number of the control points will decreased by one. The new control points set is represented by $Q = (Q_1, \dots, Q_{n-1})$. The new control points and weights can be derived from the original ones with following formulas.[3]

$$Q_i^w = P_i^w, \quad i = 1, \dots, r - p - 1 \quad (2.15)$$

$$Q_{i-1}^w = P_i^w, \quad i = r, \dots, n \quad (2.16)$$

For $r - p \leq i \leq r - 1 - p/2$

$$Q_i^w = \frac{P_i^w - (1 - \alpha_i)P_{i-1}^w}{\alpha_i}, \quad \alpha_i = \frac{u_r - u_{i+1}}{u_{i+p+2} - u_{i+1}} \quad (2.17)$$

For $r - 1 - \frac{p}{2} \leq j \leq r - 2$

$$Q_j^w = \frac{P_{j+1}^w - \alpha_j P_{j+2}^w}{1 - \alpha_j}, \quad \alpha_i = \frac{u_r - u_{j+1}}{u_{j+p+2} - u_{j+1}} \quad (2.18)$$

With the generated control points and weights, the process of knot removal is accomplished as a new NURBS curve generated. Similar to the knot insertion, the knot removal algorithm is also a very useful tool during the NURBS mesh adjusting process in IGA. However, the knot removal algorithm cannot always ensure that the shape of the newly generated NURBS curve is exactly preserved each time after a knot is removed. For example, there is a segment in a curve with a relatively complicated shape, requiring at least three control points to be precisely represented. We cannot expect that after a knot in the interval of this segment is removed, the original shape can still be precisely represented with only two control points. For the global view, the overall geometry is still preserved while utilizing the knot insertion algorithm. The change to the curve shape is restricted to the local segment.

2.4.3 Algorithms implementation to NURBS surface

As NURBS surface is the tensor product of two NURBS curves in two different directions, the two algorithms acted on curve can be easily extended to surface.

Consider a NURBS surface with the general representation defined in section 2.3.1. When a u -knot is inserted to a knot span $[u_k, u_{k+1}] \times [v_l, v_{l+1}]$, the knot insertion algorithm is applied to the entire knot span along v -direction $[u_k, u_{k+1}] \times [v_{q+1}, v_s]$. The knot insertion algorithm, demonstrated in Section 2.4.1 for the NURBS curve, is applied $s - (q + 1)$ times here. In fact, $s - (q + 1)$ is the number of control points along v -direction. Therefore, for a u or v knot insertion for NURBS surface, the process amounts to applying the knot insertion algorithm to rows or columns of control points.

The implementation of the knot removal algorithm to NURBS surface is also a process of applying of the knot removal algorithm for NURBS curve. It is exactly the same procedure in logic as the knot insertion implementation described above.

CHAPTER 3

MULTI-PATCH NURBS SURFACE ADJUSTING PROCESSOR

CAD models typically use multi-patch to describe complicated geometric shapes. A multi-patch model consists of multiple NURBS patches that match along boundaries with each patch representing a sub-region surface.

3.1 Data structure construction

In our data structure, an object named NURBS-patch is defined. The object stores the control parameters of a single NURBS patch. A multi-patch NURBS model is represented as an array of NURBS-patches. In the construction of NURBS-patch, the basic control parameters, including knots vectors, control points, and weights, are stored. Further attributes of a NURBS surface, such as the partition of elements or boundaries, are derived from them. With those basic control parameters collected in NURBS-patch, two child objects are created: NURBS-curve and NURBS-element. NURBS-curve is used to store boundary of NURBS surface. Information stored by NURBS-curve includes the knot vector, control points, weights, and some further parameters which will be introduced in later sections. NURBS-element is used to stored information of elements on a NURBS surface. The element area, element edge lengths, and element nodal coordinates are stored. With those above, the basis of data structure can be formed.

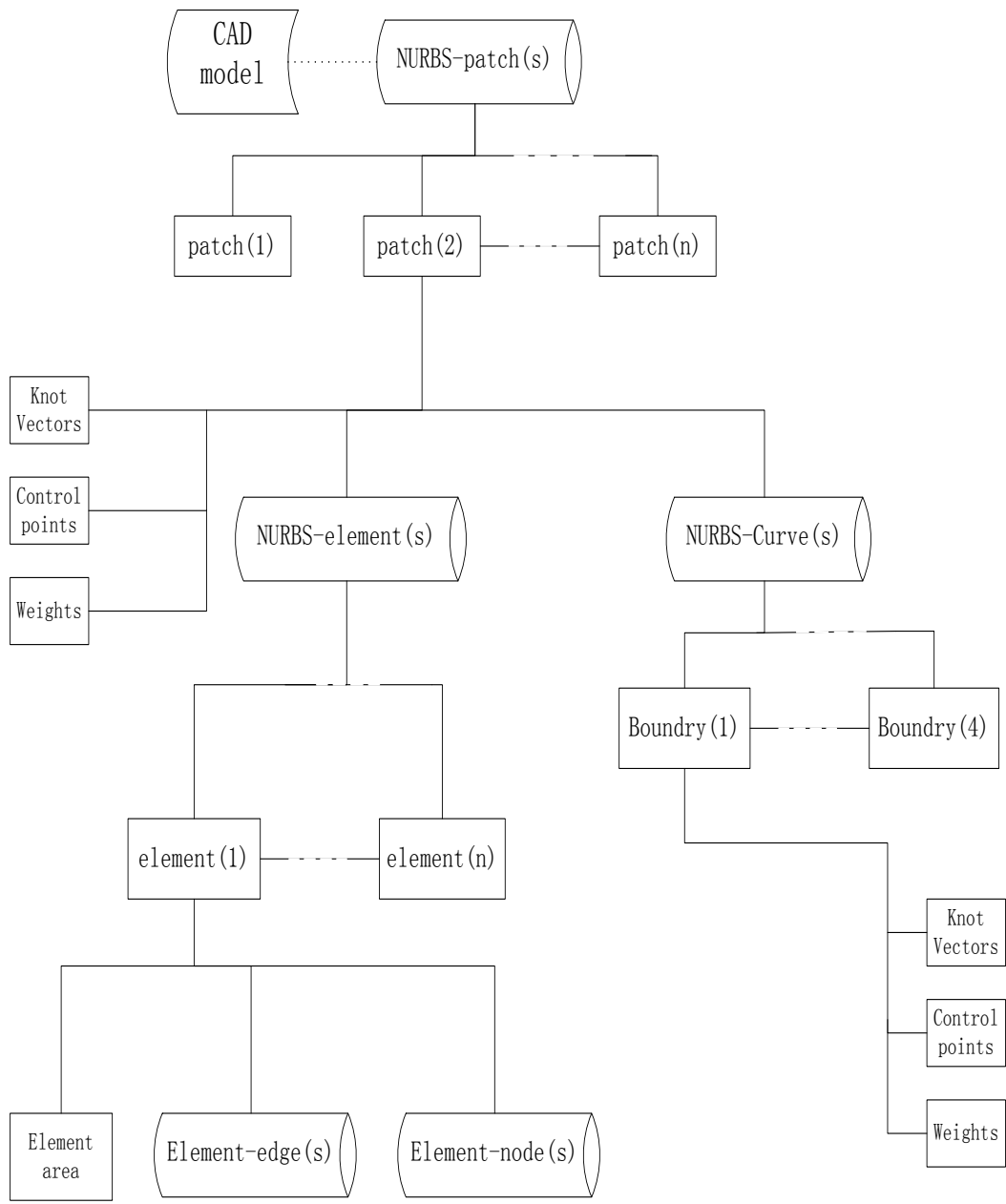


Figure 3.1: Data structure Basis

3.2 Data import and export

The original CAD is imported into our preprocessor from a file in the Initial Graphics Exchange Specification (IGES) format. IGES is used for the digital exchange of information among CAD systems, and is widely employed in industry as one of the international product data transfer standards. An IGES reader is developed to extract the information in IGES files. The knot vectors, control points, and weights of each NURBS surface recorded in corresponding character string are collected and stored in the NURBS-patch object. An IGES writer is developed to generate a new IGES file with the information from our data structure.

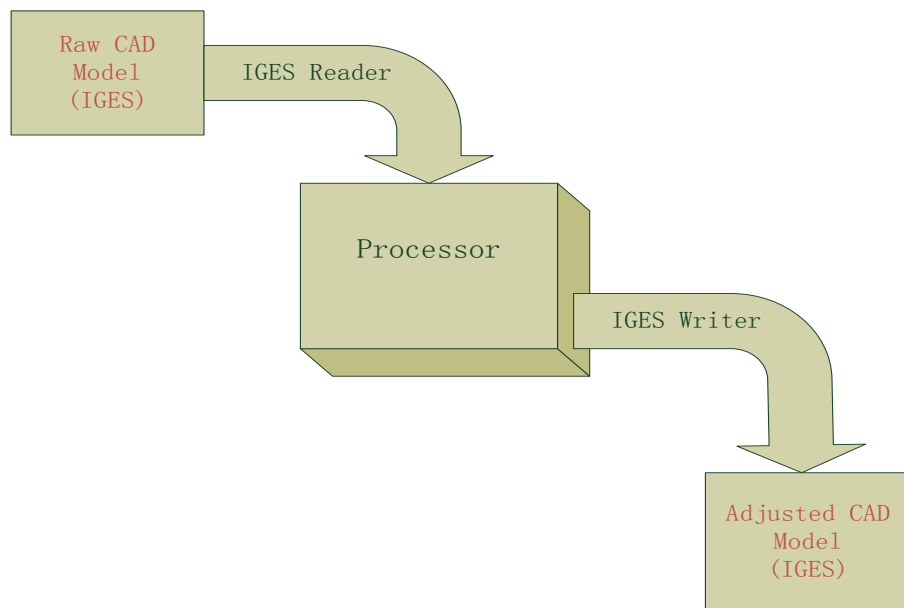


Figure 3.2: Schematic diagram of data import and export structure used in this study

3.3 Geometric computation

As mentioned in Chapter 2, a NURBS surface comes with a mesh. The original mesh in a patch is defined by knot vectors and control points. In the parametric domain, an element in a patch is determined by the tensor product of two non-empty knot spans in two knot vector directions. The four vertices appear as the element nodes in parametric space. Each element is associated with a fix number of control points (Chapter 2). All elements in the patch are numbered in order. The parametric nodal coordinates of each elements are easily collected from the knot vectors of the patch. Similarly, the corresponding control points of each elements can be extracted from the control points of the patch as well. Then, with parametric coordinate (u, v) of a node and physical coordinates of the corresponding control points $(\mathbf{P}_{i,j})$, the physical coordinates of each nodes (physical location of element node on the surface) can be derived by using the NURBS representation (p, q represent the degree order in u and v direction respectively).

$$\mathbf{S}(u, v) = \frac{\sum_{i=m}^n \sum_{j=1}^k N_{i,p}(u) N_{j,q}(v) w_{i,j} \mathbf{P}_{i,j}}{\sum_{i=m}^n \sum_{j=1}^k N_{i,p}(u) N_{j,q}(v) w_{i,j}} = \sum_{i=m}^n \sum_{j=1}^k R_{i,j}(u, v) \mathbf{P}_{i,j} \quad (3.1)$$

$$n - m = p, k - l = q$$

All nodal information is stored in the NURBS-element object. The length of each edge and the area of each element can be derived by using following formulas.

$$L = \int \left\| \frac{\partial X}{\partial u} \right\| du \quad (3.2)$$

$$\frac{\partial X}{\partial u} = \sum_{i=m}^n R_{i,p}'(u) \mathbf{P}_i \quad (3.3)$$

$$\frac{\partial X}{\partial v} = \sum_{i=m}^n R_{j,q}'(v) \mathbf{P}_j \quad (3.4)$$

$$A = \int \left| \frac{\partial X}{\partial u} \times \frac{\partial X}{\partial v} \right| dudv \quad (3.5)$$

These geometric quantities are also stored in the NURBS-element object. The knot vectors, control points, and weights of each boundary curve are extracted. Consequently, the control parameters of each boundary curve of the NURBS surface have been collected and stored under NURBS-curve in the structure.

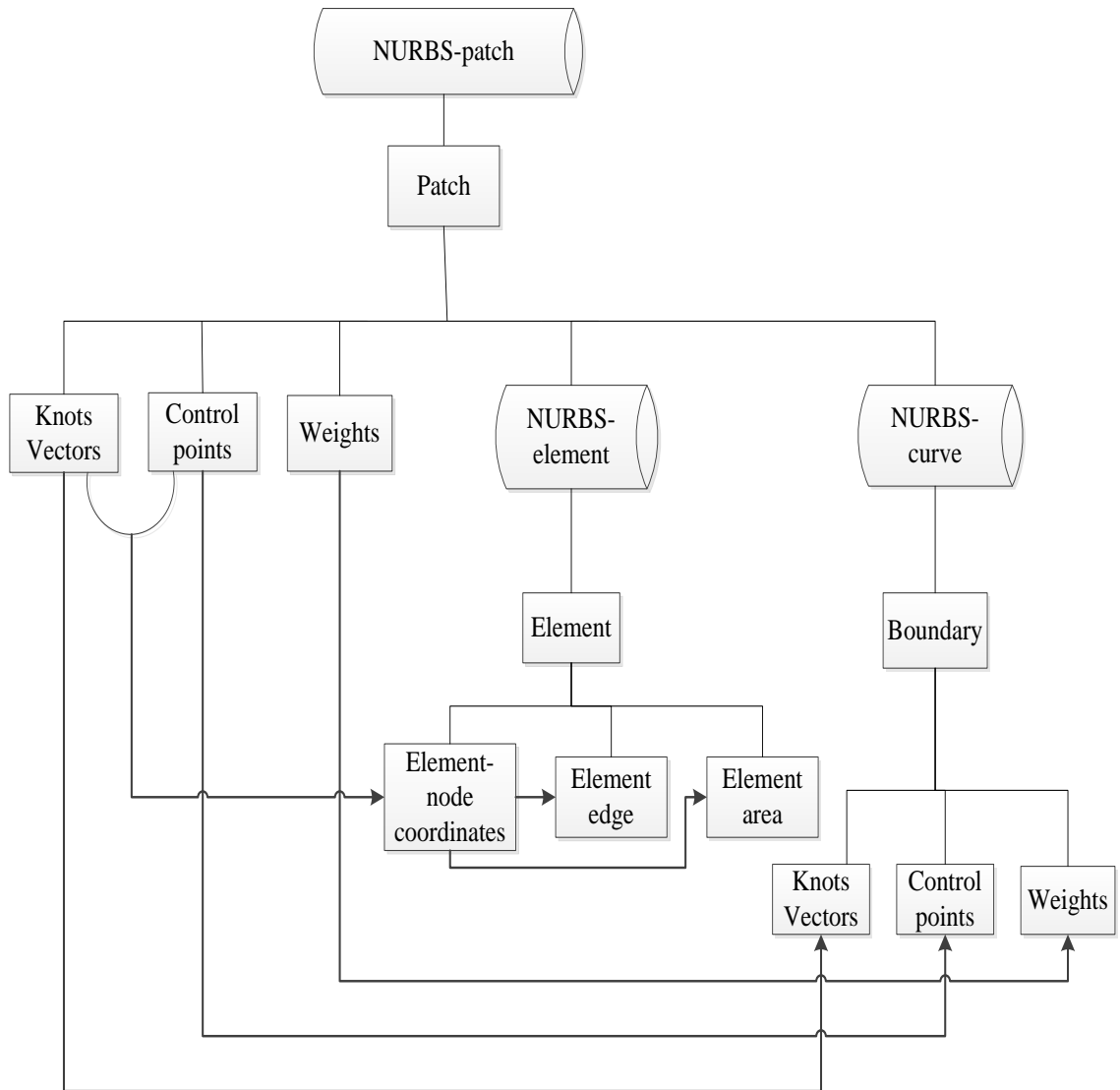


Figure 3.3: Data flow in structure

3.4 Single-patch adjusting

To demonstrate the mesh adjusting procedure, we first focus on the single-patch NURBS model. Our goal is to adjust the mesh of the NURBS surface in order to generate a relatively uniform distribution of elements in a desired element size range. For mesh adjusting, the algorithms of knot insertion and knot removal presented in Chapter 2 are applied. If the size of some elements in original mesh is too large, the knot insertion will

be performed on the corresponding knot span. On the other hand, if the size of elements in some part of the mesh is too small, some knots corresponding to the element would be removed.

3.4.1 Elements statistics

The maximum, minimum, mean, and standard of deviation of all elements area in a single patch are computed. With these information, a desired element size range can be reasonably determined. For example, one standard deviation under the mean can be made as the lower bound of desired element size range and one standard deviation over mean can be the upper bound. Based on the different situation of the original element distribution in the patch and the level of desired element size range, the choice of the lower bound and upper bound can be easily modified. The statistic process is to assist users to determine their desired range of the overall elements size. If their desired range has been specified, users can directly input the lower bound and the upper bound.

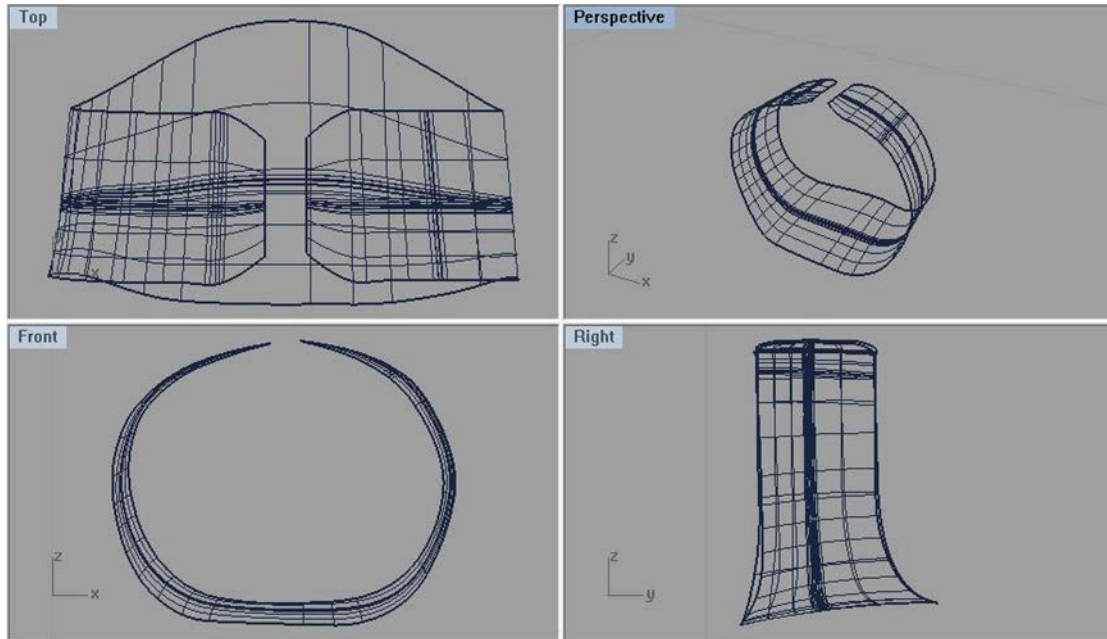


Figure 3.4: Original mesh of Single-patch model “BELT”

3.4.2 Undersize element elimination

A process of removing knots is performed to eliminate undersize elements. Using information in NURBS-element, all elements are checked one by one. The first checking index is the element area. If the area of an element does not reach the lower bound, element edge lengths need to be checked. Compared with the average element edge lengths in the two knot directions, the knots that need to be removed are decided. If the average length of element edges in U direction is smaller than the one in V direction, the knot removal algorithm will be applied to the U-knot vector. Otherwise, the knot removal will be applied on the V-knot vector. With the removal knot vector determined, the knots that will be removed can be located by checking the element nodal parametric coordinate. Then, the knot removal is applied, during which the knot vectors, control points, and weights are automatically updated. Subsequently, the child objects are updated, especially the NURBS-

element. Each time a knot is removed, the element checking process is repeated. The NURBS-patch is iteratively updated until the size of all elements is above the lower bound.

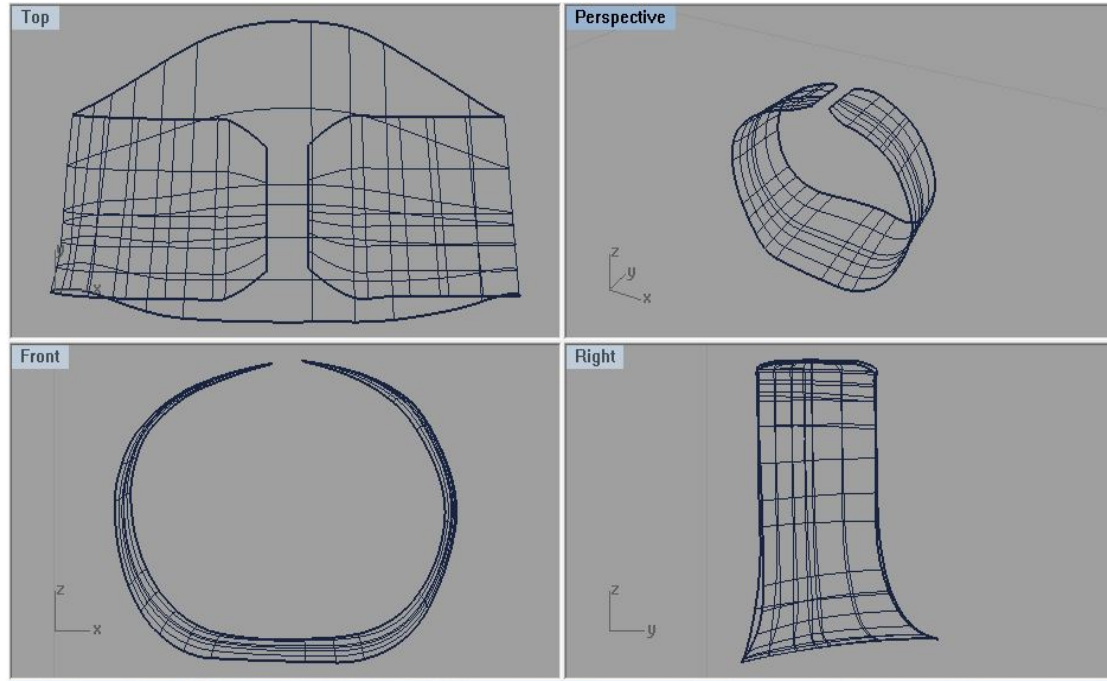


Figure 3.5: Updated mesh of Single-patch model “BELT” with undersize elements eliminated

3.4.3 Oversize element refinement

After all undersize elements are eliminated, a process of refining oversize elements is applied. The knot insertion algorithm is iteratively applied until the size of all elements is below the upper bound. The procedure is similar to the process of knot removal described in section 3.4.1. Once an element area is over upper bound, the knot insertion algorithm is applied on the direction with larger average element edges. The insertion position is in the middle of the knot span, determined by corresponding parametric nodal coordinates of the element.

With aforementioned processes completed, all elements in updated patch should satisfy the desired element size range. A new IGES file is generated. At this point, the mesh adjusting of a single-patch NURBS is completed.

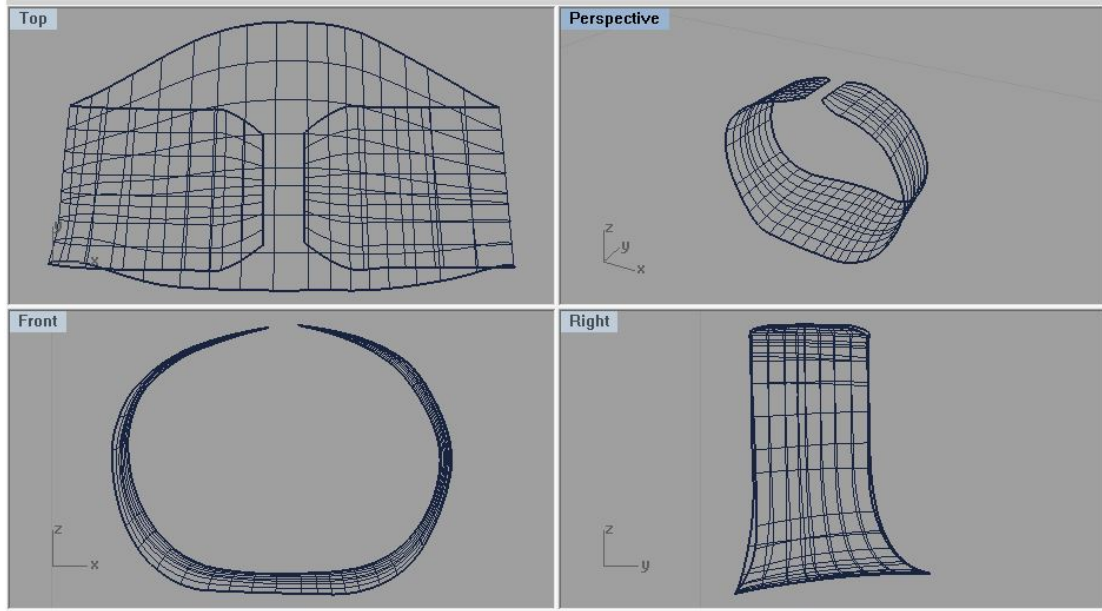


Figure 3.6: Adjusting completed mesh of Single-patch model “BELT”

3.4.4 Disparity over single-patch adjusting

Referred to Section 2.4, we have known that the knot removal algorithm may cause slightly shape change. During the single-patch adjusting process, the disparity only occurs after the process of undersize element elimination. By observing Figure 3.4-3.6, no major disparity can be captured over the overall shape of the BELT. The patch area and the number of element of each model corresponding to Figure 3.4-3.6 is represented in Table 3.1.

Table 3.1: Disparities over mesh adjusting of “BELT”

Model	Number of elements	Patch area
“Belt”-original	480	0.1691340
“Belt”-elimination	138	0.1691329
“Belt”-final output	256	0.1691329

Based on Table 3.1, the shape disparity is reflected as the change of the patch area during the adjusting process. With the whole adjusting process completed, the disparity between the patch areas of the original and final output “BELT” model is only 0.0065%.

3.5 Multi-patch adjusting

As mentioned before, CAD models typically use multi-patch to describe complicated geometries in industrial design. The mesh adjusting procedure therefore must be extended to multiple patches. To deal with multi-patch model, the connectivity among the multiple patches has to be identified in the data structure. Here, we focus on the CAD model with multiple patches that exactly match on common boundaries. At this point, it means that the element nodes and control points on the contact boundaries are the same for two adjacent patches. Later, this condition will be replaced by a distance criterion.

3.5.1 Contact Searching

In the data structure, a multi-patch NURBS model is represented as an array of NURBS-patches. In the NURBS-patches, the boundaries are stored as NURBS-curves. The edges of each patch are numbered from 1 to 4. Edges 1 and 3 have the U-knot vector. Edges 2 and 4 have the V-knot vector.

First, a contact search is performed to all boundaries in the array of NURBS-patch. The searched entity is the control points of each edge. Once the physical coordinates of the control points of two boundaries are the same, the corresponding patches must exactly match along the boundaries. A new family of NURBS boundary curve named contacted-boundary is generated in data structure as NURBS-curve object. The contacted-boundary is used to store the information of the common edges. After the searching process is

completed, for each boundary which has a contacted boundary, the contacted boundary number and its parent patch are recorded in the contacted-boundary in the data structure.

With the contact information collected for each boundary, the contact information for each patch can be derived. Another new parameter named patch-contacted is generated under NURBS-patch to store the contact information of each patch. For a patch, the contact situations can have two modes, contact in U-knot vector or V-knot vector. Consequently patches in contact with others can be divided into two groups, Uknot-contacted and Vknot-contacted, and each will collect the information of contacted patches along U-knot vector and V-knot vector, respectively. The information for each contacted patch includes the numbering of the contacted patch and the contact mode (U-contact or V-contact). U-contact and V-contact represent the contact boundary in the contacted patch is along its U-knot vector and V-knot vector, respectively.

So far, a process of contact searching is completed. For each patch with contacted patch or patches along its U-knot vector or V-knot vector, the essential information of its contacted patches will have been stored in Patch-contacted.

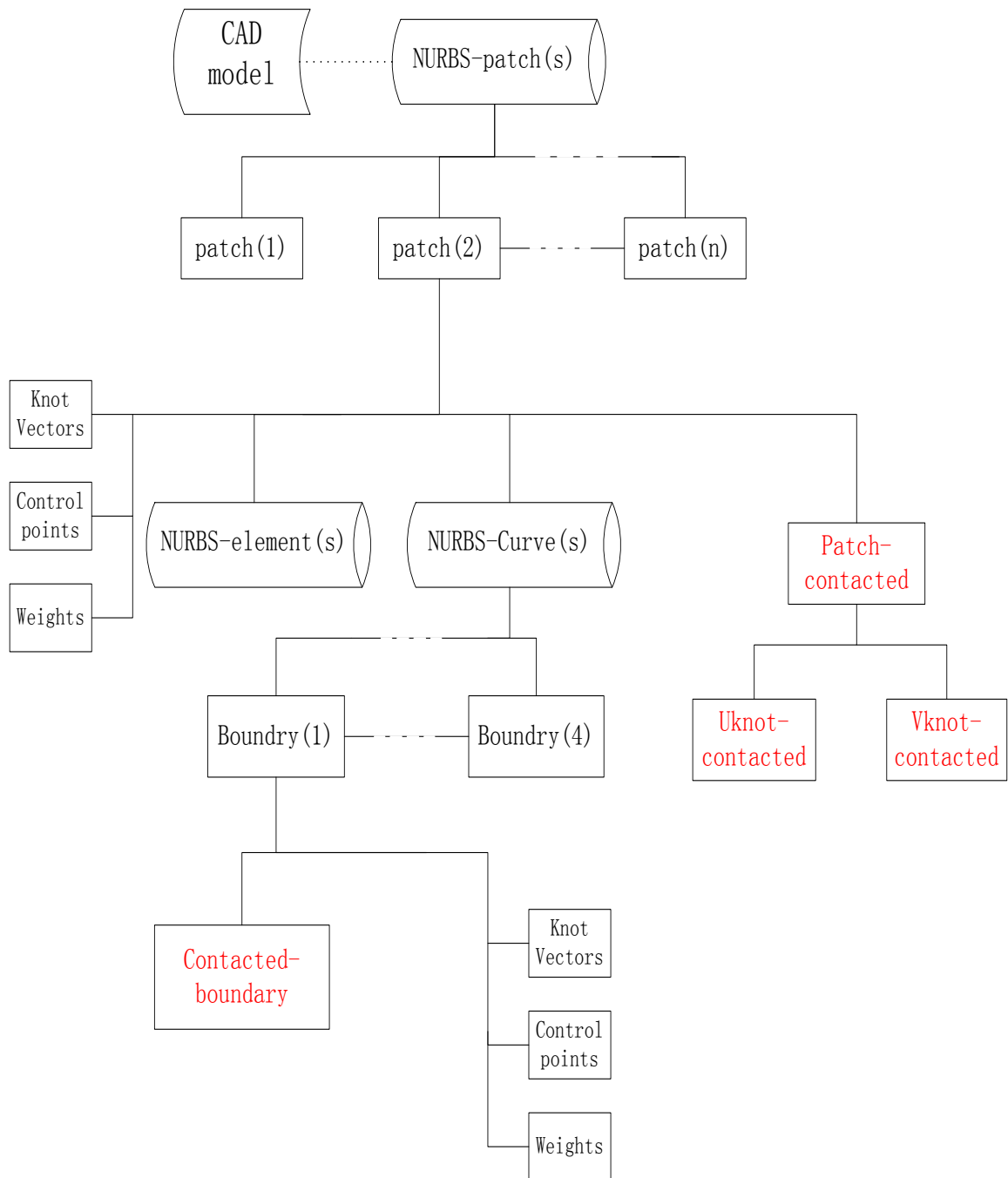


Figure 3.7: New parameters developed in Data Structure after contact searching

3.5.2 Multi-patch tree construction

Before processing multi-patch model for mesh adjusting, it is necessary to build a multi-patch tree to demonstrate the connectivity among multiple patches in the model. Another new object named Patch-tree is generated under the NURBS-patch patch, and it contains two categories named Uknot-tree and Vknot-tree defining the connection to a series of patches developed from Uknot-contacted and Vknot-contacted, respectively.

To demonstrate the process of Patch-tree construction of each patch, we randomly take a patch from the array of NURBS-patch. Each level of Patch-tree always consists of two contents, the numbering of a patch and a contact mode, which has a same form as Patch-contacted. The first level of Patch-tree is filled with the numbering of this patch and the contact mode consistent with the category of Patch-tree. For example, if we are constructing Uknot-tree of patch (1), then the first level of Uknot-tree should store numbering 1 and U-contact. Before constructing the second level, Patch-contacted of a patch needs to be checked. The numbering of the checked patch and the checked category of Patch-contacted are consistent with the ones stored in Level 1. If the corresponding category of the Patch-contacted comes with a null value, then the Patch-tree end with the first level, which means this patch has no contact with any other patch in the multi-patch model. Otherwise the second level is filled with the contents stored in the Patch-contacted. Taking the same example as above, before constructing the second level of Uknot-tree of patch (1), Uknot-contacted of patch (1) needs to be checked. We assume that Uknot-contacted of patch (1) stores patch (6) with V-contact and patch (7) with U-contact, then the second level of Uknot-tree should be refilled with these two sets of data. From the second level, before constructing each upper level, the Patch-contacted object of its parent patch and the category determined by the contents stored in current level are checked

together with all data sets that have been generated in all of the lower levels. Once a data set in the Patch-contacted object comes out to have already appeared in lower levels, it is skipped. If every data set in the Patch-contacted object comes to be a repeat or a null value, level construction stops by current level. Up to this point, Patch-tree construction of a patch is completed.

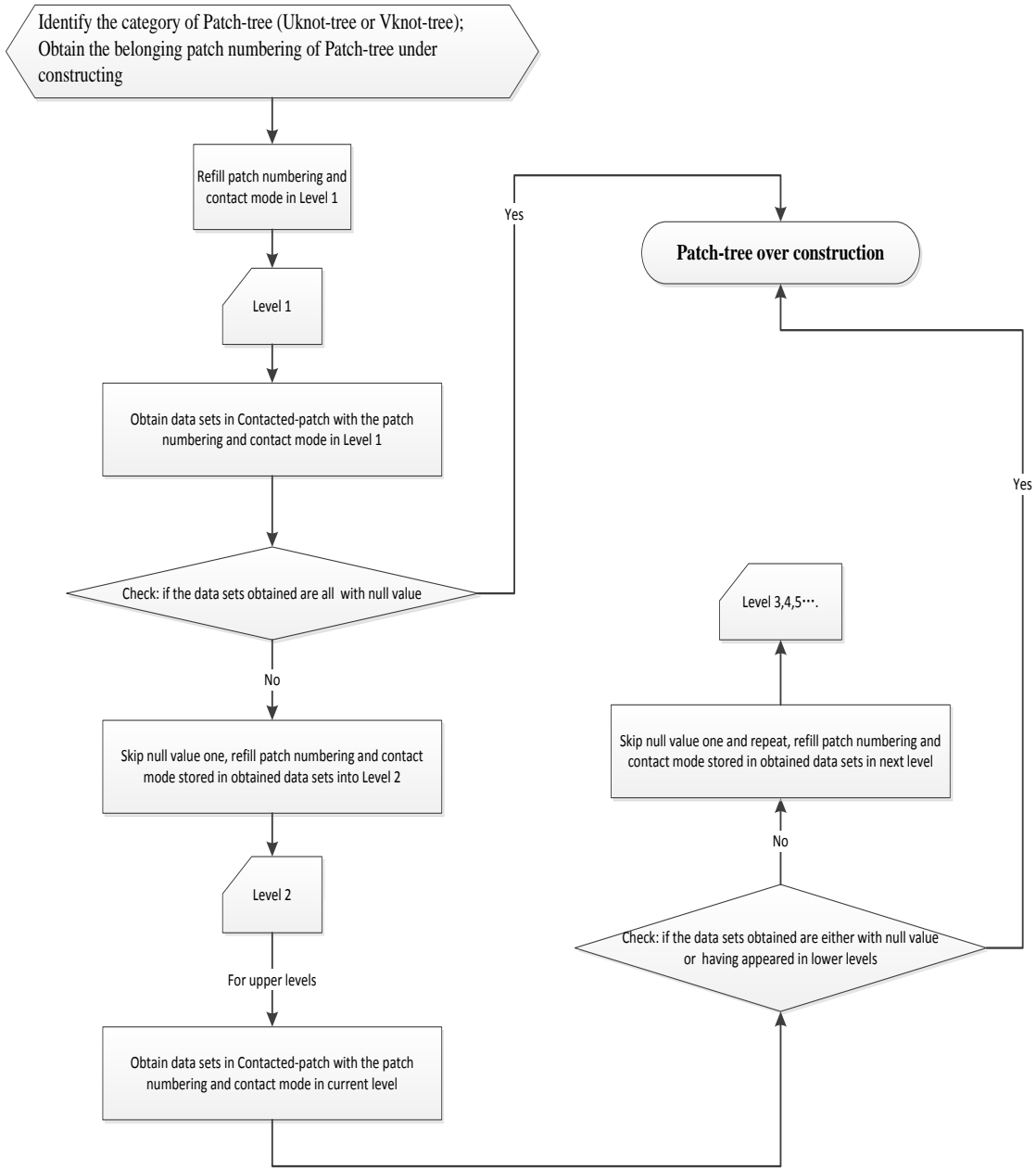


Figure 3.8: Flow chart of Patch-tree construction

When the process of Patch-tree construction has been performed over all patches in the array of NURBS-Patch, an invisible multi-patch tree has been generated. All essential information for defining the connectivity between patches has been stored in Uknot-tree and Vknot-tree of each patch in the data structure.

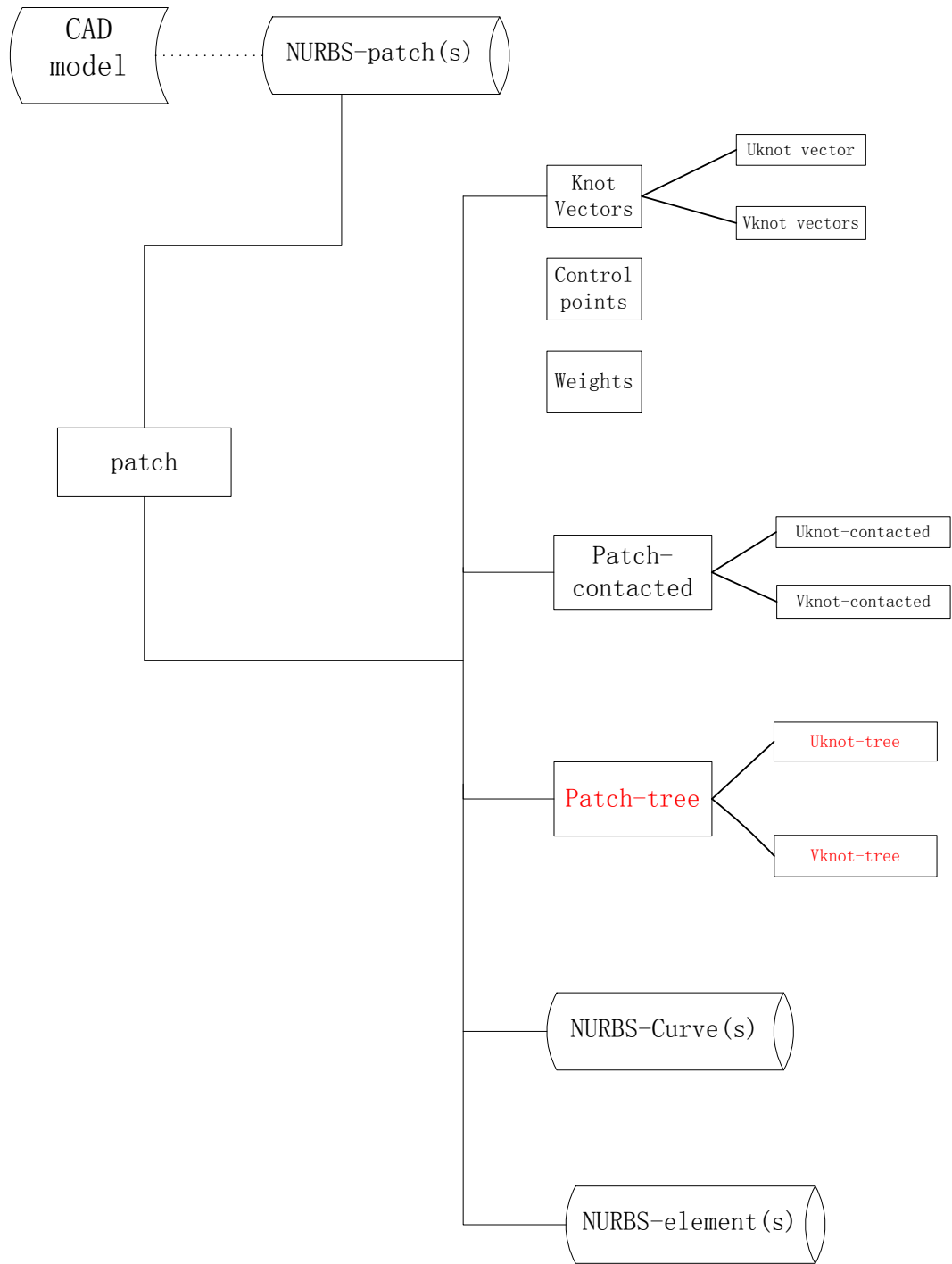


Figure 3.9: Parameters of NURBS-patch in Data structure with Patch-tree developed

3.5.3 Adjusting process

The goal for mesh adjusting in multi-patch model is the same as the one for single-patch adjusting. We are aiming at adjusting all the patches in the model so that each of them has a relatively uniformly distributed elements.

The process begins with an element geometry statistical analysis which is used to determine the upper bound and lower bound of the element size. Here, the statistical sample is the elements in all patches instead of in a single patch. In the data structure, the statistical data collection goes through the whole array of NURBS-patch, gathering the element area stored under each NURBS-element in each NURBS-patch. The mesh adjusting procedure also consists of two processes, undersize elements elimination and oversize elements refinement.

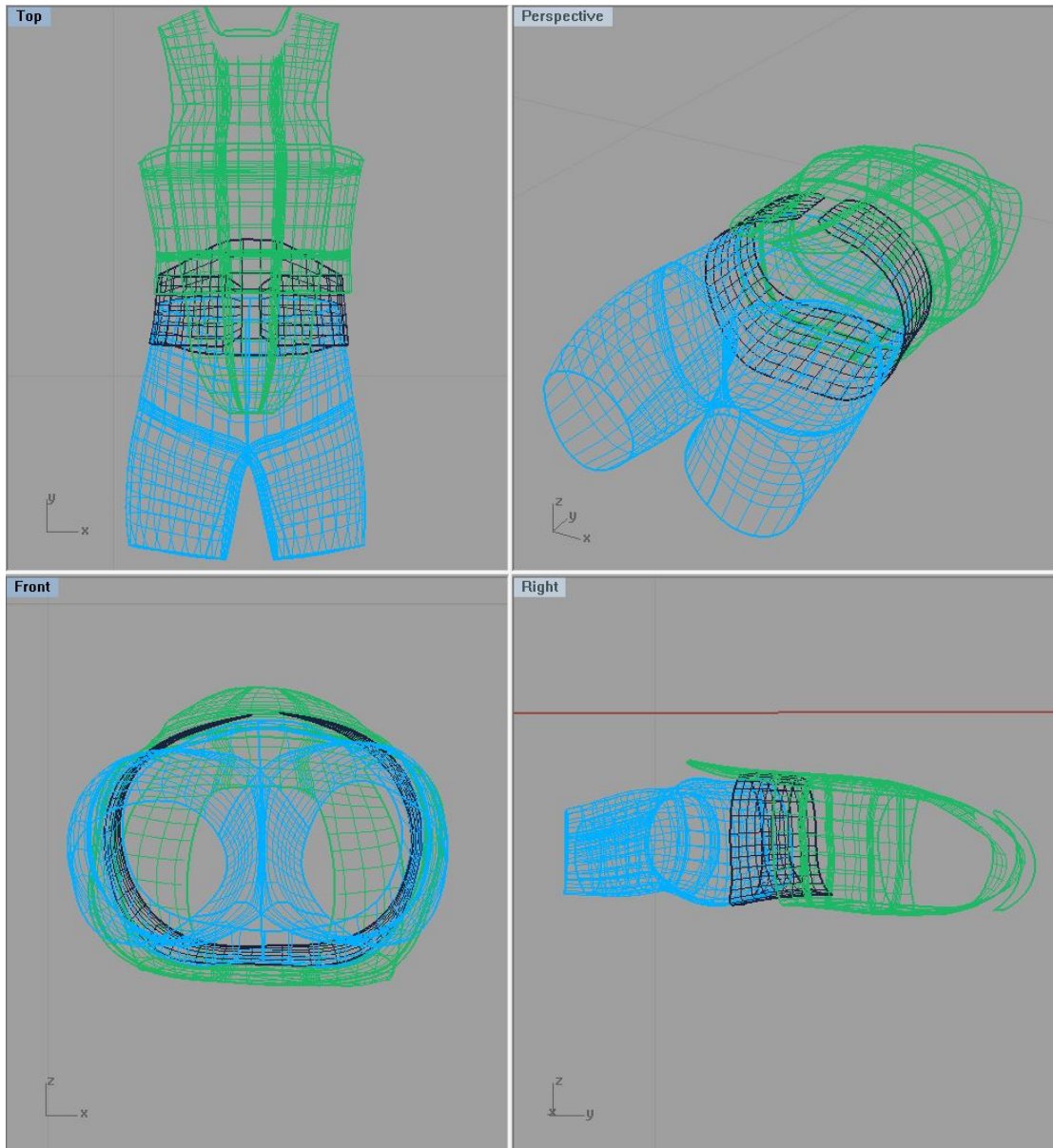


Figure 3.10: Original mesh of ideal designed (contact boundaries mesh fitted) Multi-patch model “VEST”

All patches first go through the process of undersize elements elimination. In each patch, while the location of elimination is identified in the same way as before, the removal procedure should be applied to all the objects stored in the corresponding category of the Patch-tree of current patch. For example, if a knot on U-knot vector of the current patch needs to be removed, the Uknot-tree of the current patch will be involved. The patch

number and contact mode in each set stored in the Uknot-tree indicate the Patch and its U or V-vector to which the knot removal algorithm will be applied. Since the Patch-tree is constructed based on the boundaries along which multiple patches exactly matches, all corresponding knot-vectors in the patches stored in the same category of Patch-tree must be of the same scale. When a knot in U-or V-knot vector is removed in current patch, for all the other patches which have connection with current patch in this knot vector direction, a corresponding knot for each will be removed at the same time. This ensures that the mesh of each contact patch still match along the boundary after each application of the knot removal. When all patches have gone through the process of undersize elements elimination, undersize element will no longer exist in the whole multi-patch model.

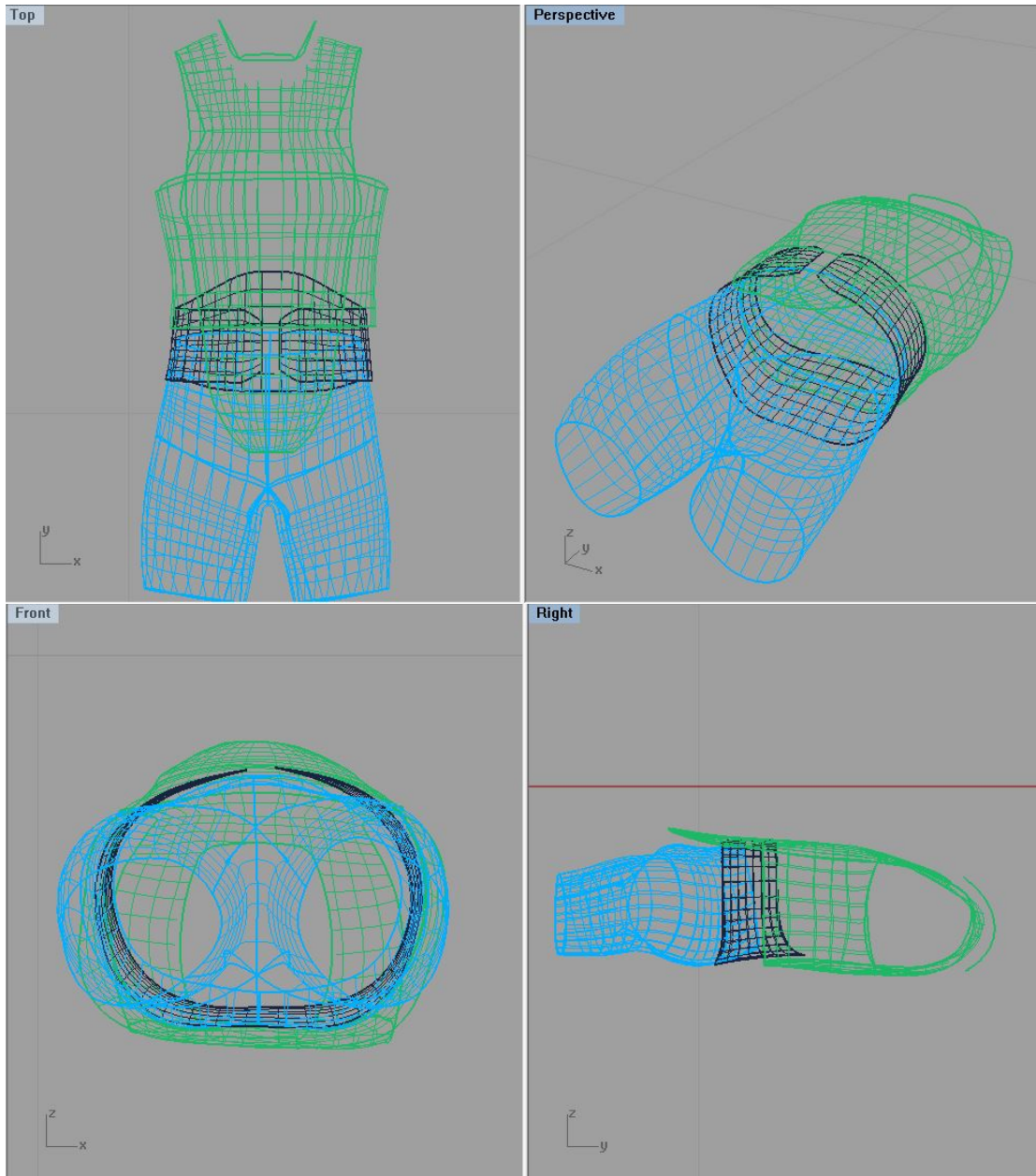


Figure 3.11: Updated mesh of ideal design Multi-patch model “VEST” with undersize elements eliminated

The process of oversize elements refinement then follows. During this process, the knot insertion algorithm is applied to an identified knot spans in the current patch and the corresponding knot spans of all patches stored in the Patch-tree of the current patch, just like the process of knot removal. With both processes (undersize elements elimination and

oversize elements refinement) completed, all elements in each patch in the Multi-patch fall into the desired element size range.

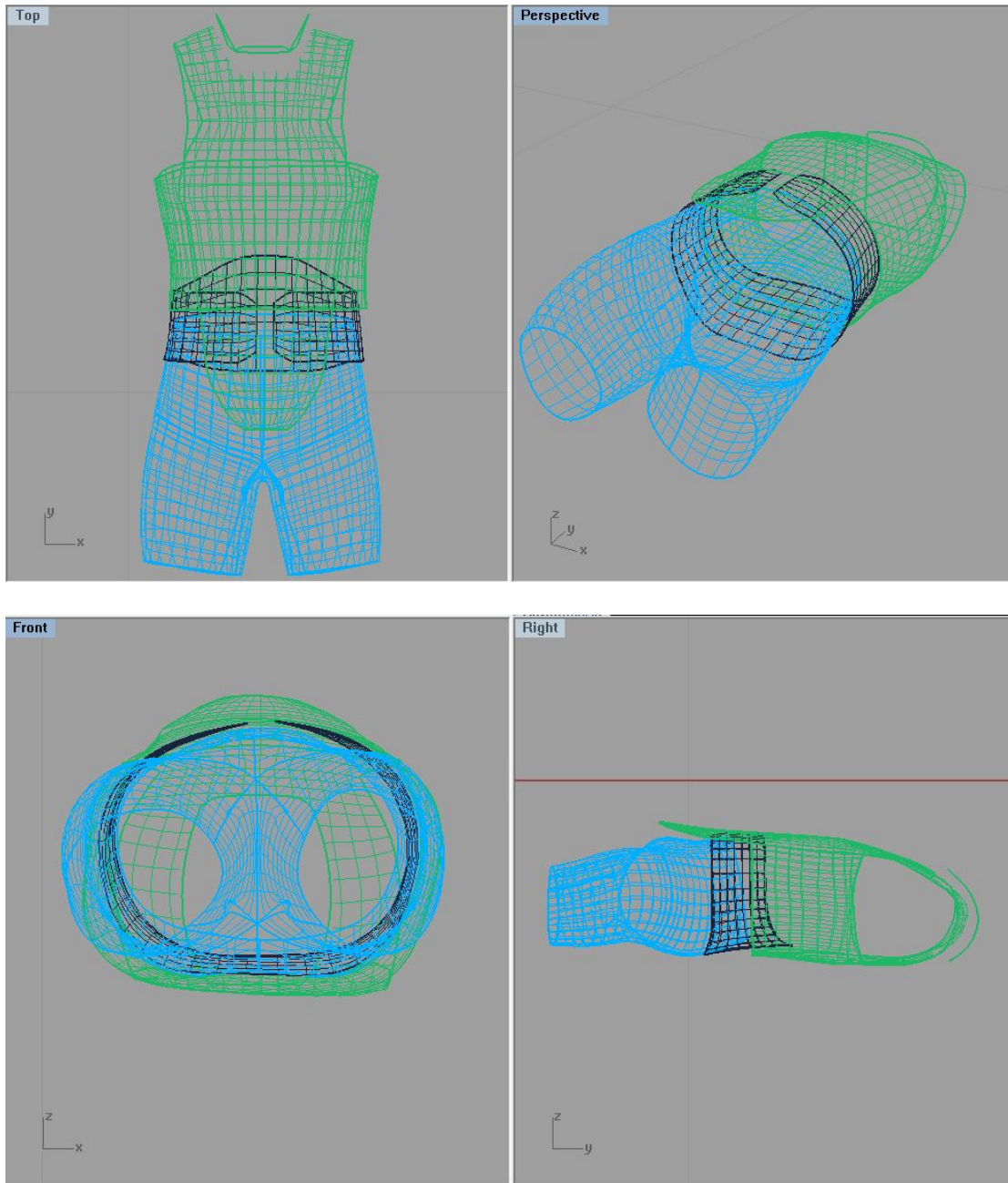


Figure 3.12: Updated mesh of ideal design Multi-patch model “VEST” with all elements in desired size range

3.5.4 Contact boundary modification

Since the knot removal cannot exactly preserve the geometry, the shape of contact boundaries in the original Multi-patch can be slightly changed after the mesh adjusting. As a result, the mesh of contact patches along the contact boundaries may not exactly match with each other anymore. In order to resolve this issue, we replace the control points of one of the contact boundaries with those of the other boundary in contact with it. After that, the element nodes on both contact boundaries will be exactly coincident in physical coordinates, ensuring that the mesh of contact patches still exactly matches along the contact boundary.

After all the sets of contact boundaries in the Multi-patch are fixed, the control point sets of their parent patches are updated. A new IGES file is then generated via IGES Writer with updated basic control parameters stored in our data structure, completing the whole process of the mesh adjustment for a Multi-patch NURBS model.

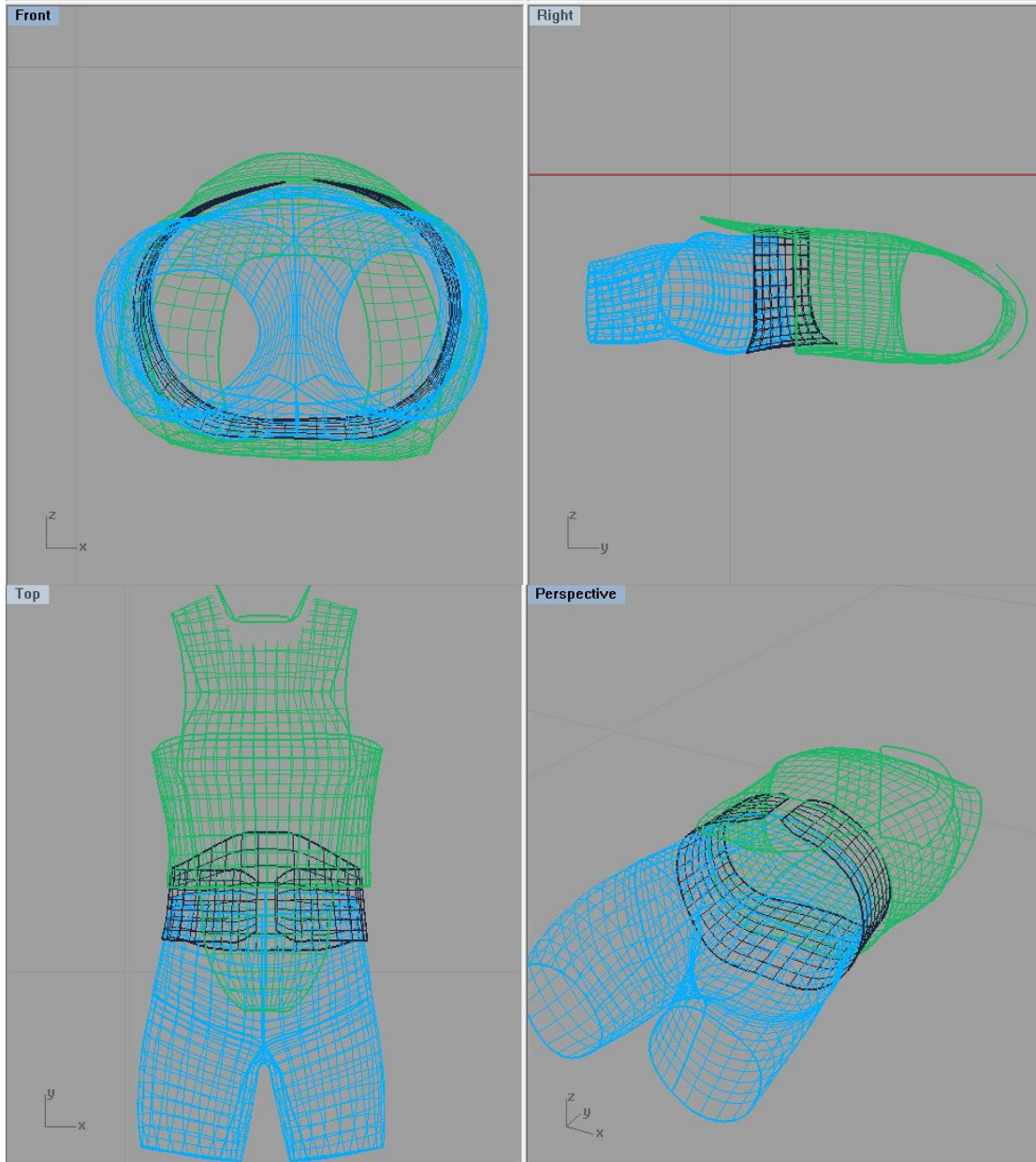


Figure 3.13: Adjusting completed mesh of ideal designed Multi-patch model “VEST” with modified contact boundaries

3.5.5 Disparity over Multi-patch adjusting

For the mesh adjusting of Multi-patch model, the disparities may occur at two places. One is right after the undersize elements elimination process due to the applications of the knot removal algorithm. The other is after the contact boundary modification at the final

step. As the control points sets of contact boundaries is synchronized, the shape of some boundaries may be slightly modified. Table 3.2 shows the disparities between the original and the final output “VEST” model based on the change of the area of corresponding patches in the two models.

Table 3.2: Disparities over multi-patch model adjusting of “VEST”

Patch Number	Original VEST model	Final output VEST model	
	Patch area	Patch area	Percentage change
1	4.2296075E-02	4.2302038E-02	0.0141%
2	6.4354915E-02	6.4363692E-02	0.0136%
3	1.1544001E-01	1.1544000E-01	0.0000%
4	2.2104623E-02	2.2163215E-02	0.2651%
5	1.6878088E-01	1.6868783E-01	0.0551%
6	9.7112150E-02	9.7112075E-02	0.0001%
7	1.3366980E-01	1.3448614E-01	0.6107%
8	7.3661465E-02	7.3670147E-02	0.0118%
9	6.3114548E-02	6.3114297E-02	0.0004%
10	6.3103686E-02	6.3103597E-02	0.0001%
11	9.6602263E-02	9.6602370E-02	0.0001%
12	1.1580950E-01	1.1580954E-01	0.0000%
13	2.2242455E-02	2.2277484E-02	0.1575%

In Table 3.2, the disparities based on the area change of each patch in the “VEST” model are all in an acceptable level (under 1%). Up to here, the evaluation of the disparity over multi-patch model adjusting, to some extent, supports that the whole adjusting process developed for Multi-patch model is feasible.

3.6 Originally mis-matched boundaries

In real world, a Multi-patch NURBS model often comes with mismatched descriptions for presumably contact boundaries. Visually contact patches may not have an exactly matching boundary, and particularly, the element nodes along the contact

boundaries of two patches may not be coincident. Accordingly, the Multi-patch adjusting process described in section 3.5 must be modified in order to handle real world models.

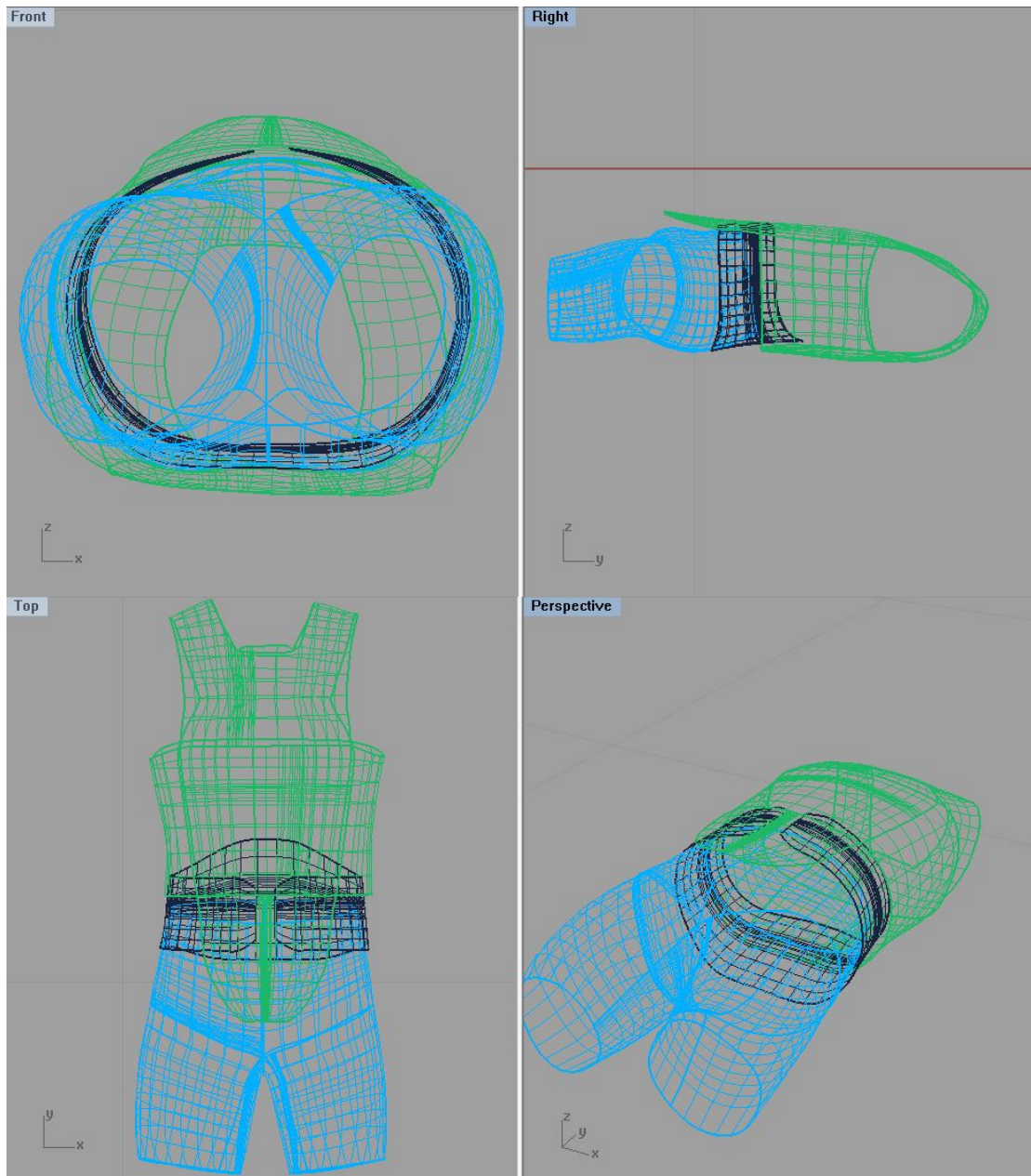


Figure 3.14: Original mesh of raw designed (contact boundaries mesh not fitted) Multi-patch model “VEST”

3.6.1 Searching criteria update

Since contact patches may not exactly match along boundary, the control points are no longer suited as identifiers while searching for contact boundaries (in section 3.5.1). The procedure is modified as follows. Before searching, three points on each boundary through the whole array of NURBS-patch are picked to calculate their physical coordinates. These three points are the beginning point, the middle point, and the end point on each boundary. For a NURBS curve, the beginning point and the end point on the boundary are the first and the last control points of the boundary curve. The physical coordinates of the middle point are derived with the middle knot coordinate of the knot vector (u) and its corresponding control points(\mathbf{P}_i) using NURBS interpolation (p represents a p -th order degree).

$$\mathbf{C}(u) = \frac{\sum_{i=m}^n N_{i,p}(u)w_i\mathbf{P}_i}{\sum_{i=m}^n N_{i,p}(u)w_i} = \sum_{i=m}^n R_{i,p}(u)\mathbf{P}_i \quad (3.6)$$

$$n - m = p$$

The physical coordinates of these three points are stored as a new parameter of each boundary. Thereupon, searching for contact boundary can be performed. During searching, if sum of the distances between corresponding points on two boundaries among the three points is less than a threshold, these two boundaries are considered as matching. Although matching at only three points is far from enough to ensure a matching along the curve, in real world, this method can still be utilized as an indicator to categorize the presumably contact boundaries for multi-patch NURBS models. Under some extreme circumstance, the number of the points as the identifiers on a curve can be increased.

With such updated searching criteria, the process of Contacted Searching and Multi-patch tree Construction, as described in Sections 3.5.1 and 3.5.2, can be applied on raw designed Multi-patch model.

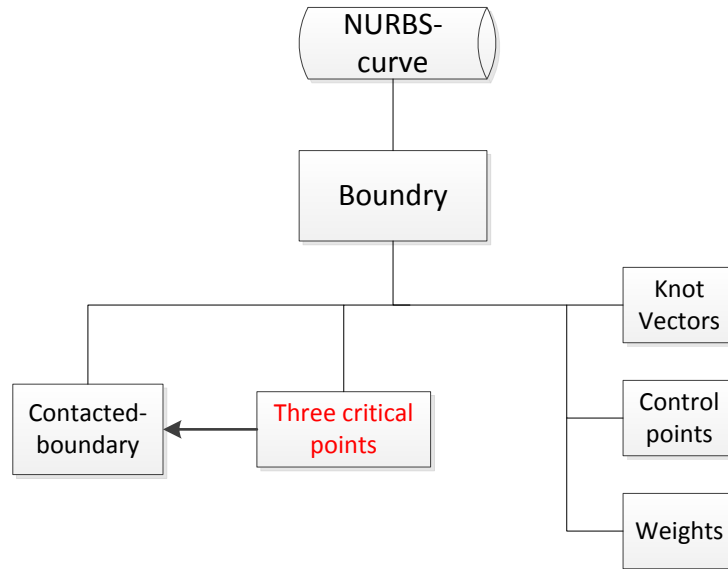


Figure 3.15: New parameter of NURBS-curve developed for updated searching criteria

3.6.2 Knots synchronization over contact patches

Before applying the adjusting process (3.5.3), a process called knot synchronization needs to be performed for the raw designed Multi-patch model, since the knot vectors in a contacted direction of the two adjacent patches may not have the same parameterization. The knots synchronization is introduced to homogenize the knot parameters over the common edge. The achievement of knots synchronization is based on the Patch-tree of each patch. For U or V-knot vectors of the current patch, we compute a set of knots for corresponding knot vector of each patch recorded in Patch-tree. The computed sets of knots divides each corresponding knot vector to the same proportion segments as the one of current patch. After that, we apply knot insertion to insert those sets of knots into corresponding knot vectors. Each time after a knot insertion is completed, all

corresponding parameters of the patch, such as knots vectors, control points set, elements etc., get updated immediately. After this process has been performed from the first to the last patch in the model (NURBS-patch array in data structure), the knot vectors of all patches in a same contacted direction will have one to one correspondence.

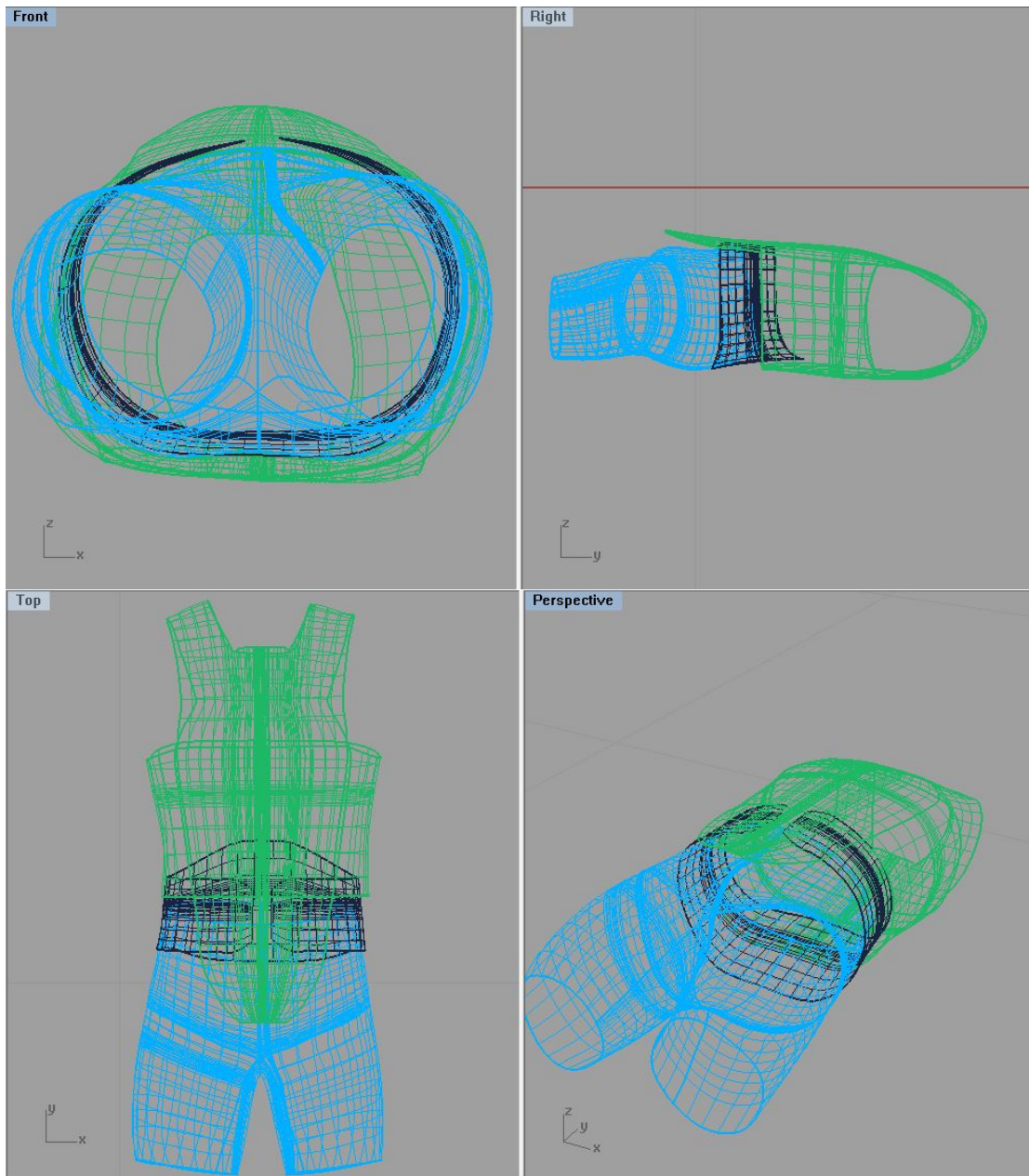


Figure 3.16: Updated mesh of raw designed Multi-patch model “VEST” with knots synchronized over contact patches

Up to this point, the processes described in Sections 3.5.3 and 3.5.4 can then be applied to complete mesh adjusting over raw designed Multi-patch NURBS model.

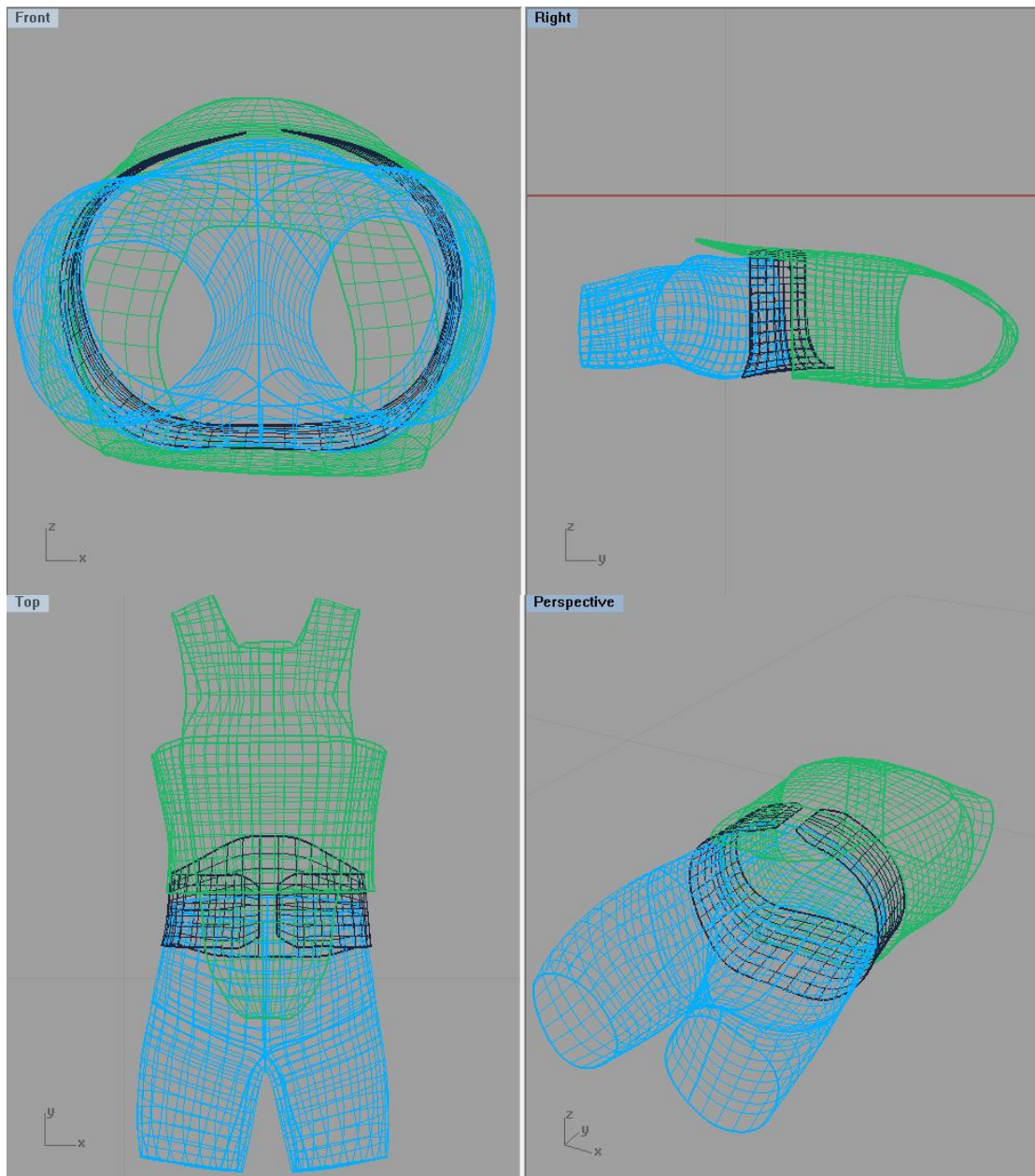


Figure 3.17: Adjusting completed mesh of raw designed Multi-patch model “VEST”

CHAPTER 4

APPLICATION ON RAW CAD MODEL

In real CAD design, the original CAD model usually is not design-intended. The model can have a huge amount of elements in some patches, or can have vastly heterogeneous element size. Such models are typically not directly usable for analysis. An application of our processor processed with an over dense mesh CAD model is presented in this Chapter.

4.1 Description of original CAD model

The original CAD model is a body armour described by multiple NURBS patches. Some of the patches matches along patch boundaries, while some of them matches along trimmed boundaries. The model contains 52 patches and 45054 elements in total. Some of the patches have over 5000 elements which is overly dense. The original mesh of the entire body armour is shown in Figures 4.1 and 4.2. Figure 4.3 shows a zoom in perspective of a part of the suit sleeve which is a typical overly dense mesh reflect. Our goal is to adjust the CAD model to render a reasonable element distribution for each patch. In addition, the mesh of the contact patches which originally matches along patch boundaries is ensured to remain matched along contact boundary.

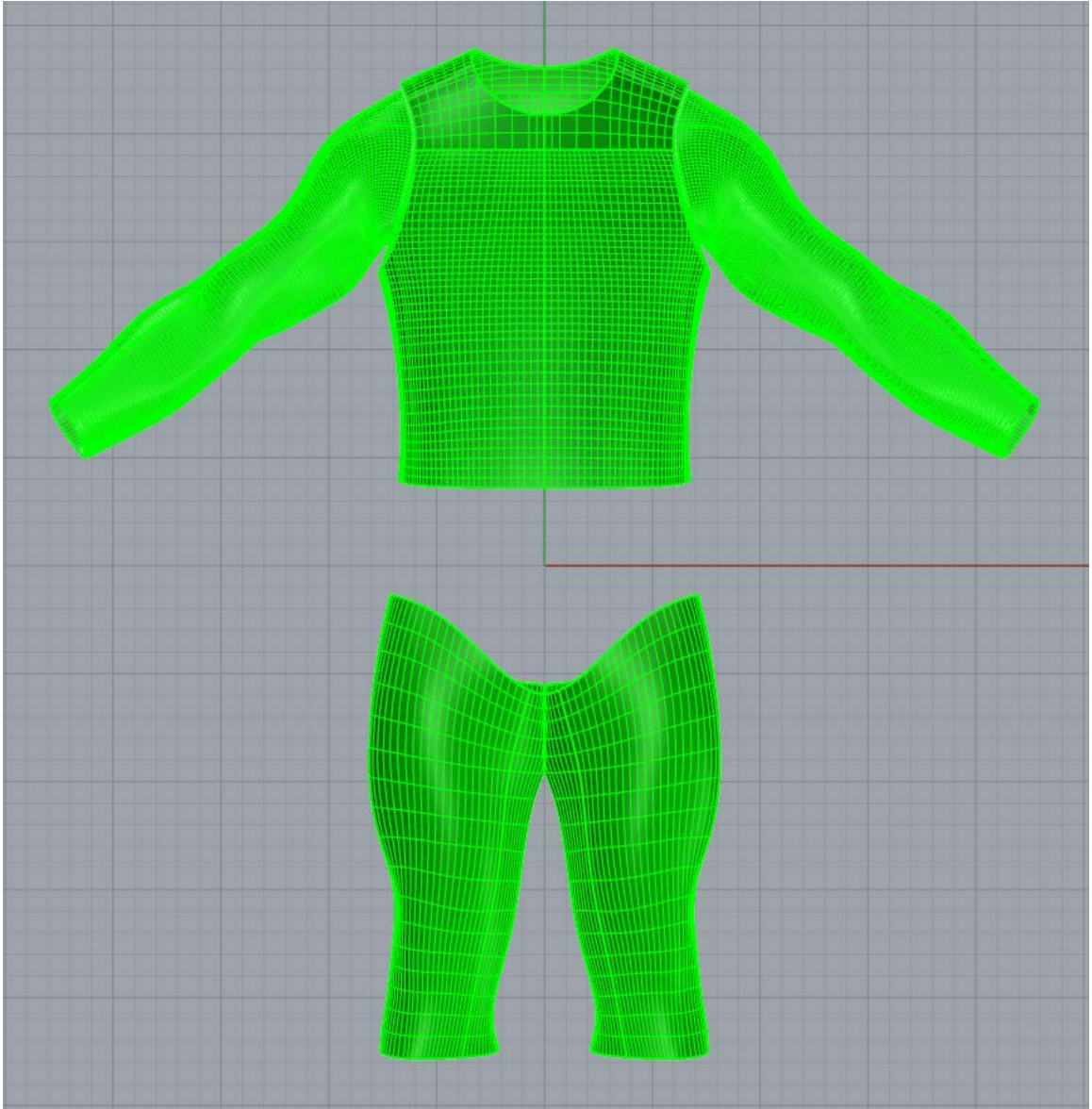


Figure 4.1: Front vision of original mesh of body armour

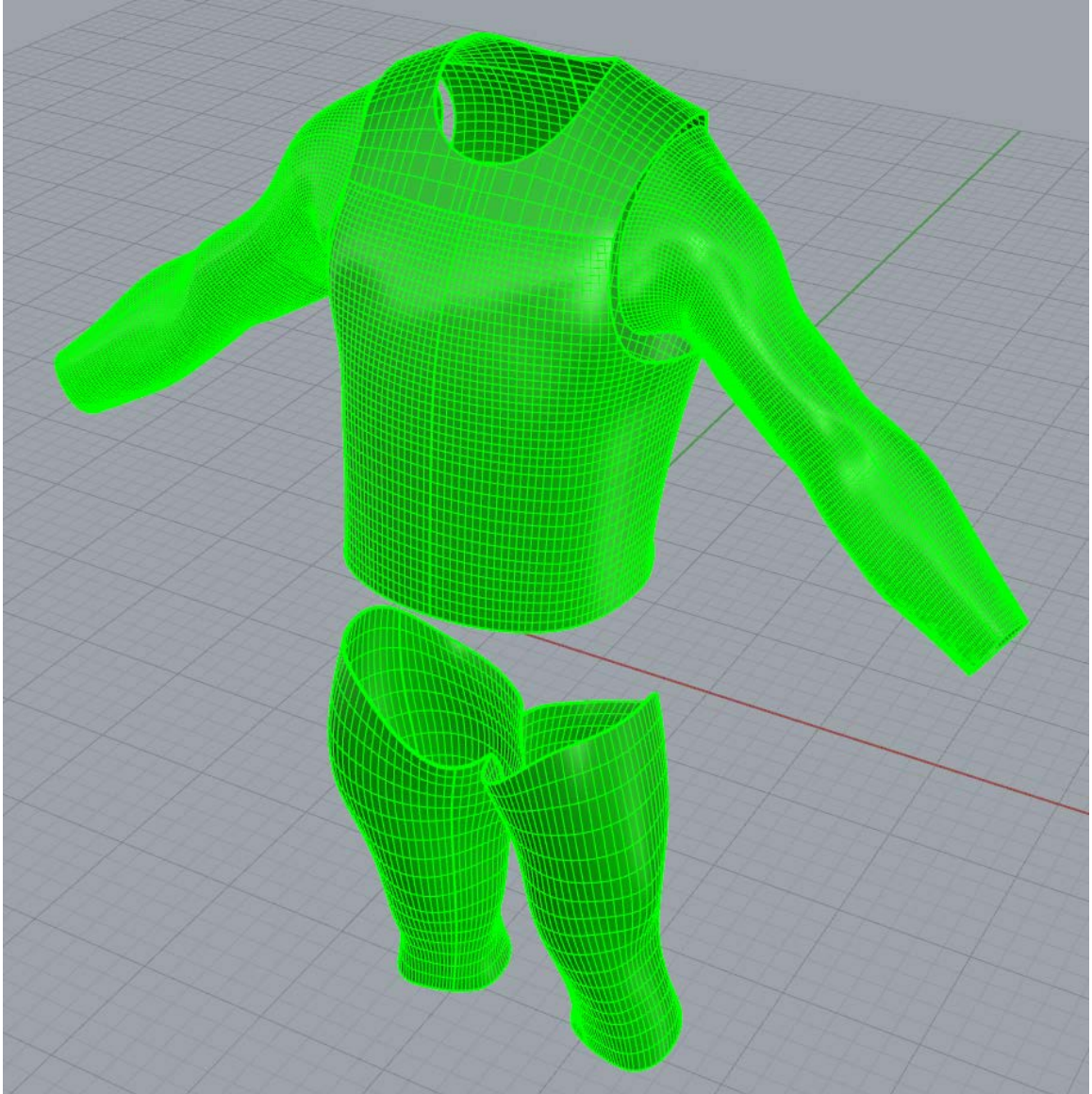


Figure 4.2: Perspective vision of original mesh of body armour

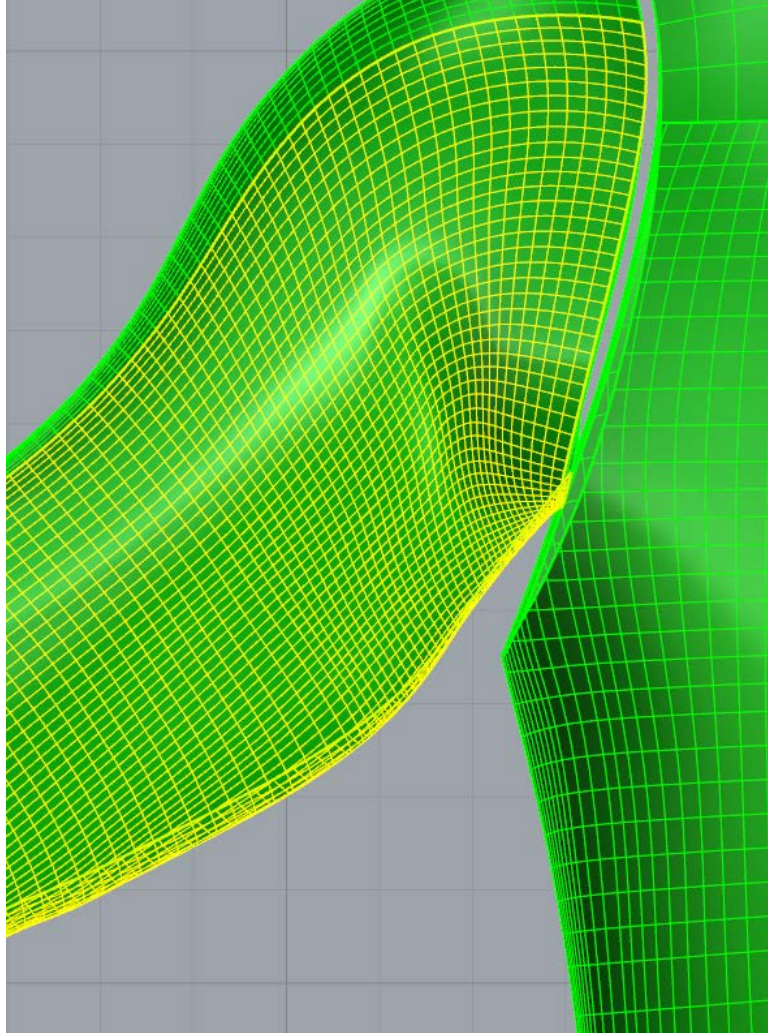


Figure 4.3: Sleeve zoom in of original mesh of body armour

4.2 Statistics on original mesh of body armour

The original model is imported to our data structure through IGES Reader. Before the adjusting process, a basic statistical data are collected on the original mesh of body armour. The total area, the number of elements, and the element mean area of each patch are obtained. Table1 lists above information of each patch with a patch number consistent with the numbering in our data structure.

Table 4.1: Summary of patches information on original mesh of body armour

Patch Number	Elements	Patch Area	Element Area Mean
1	864	169.338	1.96E-01
2	30	0.482	1.61E-02
3	33	1.209	3.66E-02
4	5529	182.329	3.30E-02
5	800	141.790	1.77E-01
6	29	0.487	1.68E-02
7	28	1.221	4.36E-02
8	5529	149.833	2.71E-02
9	646	241.084	3.73E-01
10	714	203.654	2.85E-01
11	43	0.912	2.12E-02
12	6	0.220	3.66E-02
13	68	2.451	3.61E-02
14	714	199.722	2.80E-01
15	646	247.561	3.83E-01
16	41	0.846	2.06E-02
17	135	2.480	1.84E-02
18	714	199.722	2.80E-01
19	646	247.561	3.83E-01
20	41	0.846	2.06E-02
21	6	0.220	3.66E-02
22	68	2.451	3.61E-02
23	646	241.084	3.73E-01
24	714	203.654	2.85E-01
25	43	0.912	2.12E-02
26	135	2.480	1.84E-02
27	800	141.790	1.77E-01
28	29	0.487	1.68E-02
29	28	1.221	4.36E-02
30	5529	149.833	2.71E-02
31	864	169.338	1.96E-01
32	30	0.482	1.61E-02
33	33	1.209	3.66E-02
34	5529	182.329	3.30E-02
35	2646	410.421	1.55E-01
36	299	70.846	2.37E-01
37	2646	410.421	1.55E-01
38	276	70.123	2.54E-01
39	480	71.304	1.49E-01
40	2816	381.491	1.35E-01

Table 4.1-continued

41	63	0.767	1.22E-02
42	87	1.077	1.24E-02
43	75	1.008	1.34E-02
44	81	0.844	1.04E-02
45	138	1.802	1.31E-02
46	480	71.304	1.49E-01
47	2816	381.491	1.35E-01
48	63	0.767	1.22E-02
49	87	1.077	1.24E-02
50	75	1.008	1.34E-02
51	81	0.844	1.04E-02
52	135	1.782	1.32E-02

Table 4.1 is re-arranged as an order of increasing quantity of elements of each patch. Through a rough analysis of current quantity of elements and element area mean, a criterion of lower bound is generated for the later process of undersize elements elimination (Sections 3.4.1 and 3.4.2). The objective is to reduce the element number in each patch to around 200 or less after the process of undersize elements elimination. Table 4.2 summarizes the criterion to make the lower bound for each patch based on its original elements number and element area mean.

Table 4.2: Lower Bound Standard

Elements number	Lower Bound
1 to 100	Area Mean
101 to 200	1.5*Area Mean
201 to 500	3*Area Mean
501 to 1200	6*Area Mean
1201 to 3000	12*Area Mean
Over 3000	24*Area Mean

Table 4.3 is the re-arranged and updated version of Table 4.1 with lower bound of each patch determined. By inspecting the patch area and lower bound ratio of each patch in the table, we can then reasonably conclude that the number of elements in each patch will not significantly exceed 200 after later process of undersize elements elimination.

Table 4.3: Updated Patches information with Lower Bound

Patch Number	Elements	Patch Area	Element Area Mean	Lower Bound	Patch Area/ Lower Bound
12	6	0.220	3.66E-02	3.66E-02	6.0E+00
21	6	0.220	3.66E-02	3.66E-02	6.0E+00
7	28	1.221	4.36E-02	4.36E-02	2.8E+01
29	28	1.221	4.36E-02	4.36E-02	2.8E+01
6	29	0.487	1.68E-02	1.68E-02	2.9E+01
28	29	0.487	1.68E-02	1.68E-02	2.9E+01
2	30	0.482	1.61E-02	1.61E-02	3.0E+01
32	30	0.482	1.61E-02	1.61E-02	3.0E+01
3	33	1.209	3.66E-02	3.66E-02	3.3E+01
33	33	1.209	3.66E-02	3.66E-02	3.3E+01
16	41	0.846	2.06E-02	2.06E-02	4.1E+01
20	41	0.846	2.06E-02	2.06E-02	4.1E+01
11	43	0.912	2.12E-02	2.12E-02	4.3E+01
25	43	0.912	2.12E-02	2.12E-02	4.3E+01
41	63	0.767	1.22E-02	1.22E-02	6.3E+01
48	63	0.767	1.22E-02	1.22E-02	6.3E+01

Table 4.3-continued

13	68	2.451	3.61E-02	3.61E-02	6.8E+01
22	68	2.451	3.61E-02	3.61E-02	6.8E+01
43	75	1.008	1.34E-02	1.34E-02	7.5E+01
50	75	1.008	1.34E-02	1.34E-02	7.5E+01
44	81	0.844	1.04E-02	1.04E-02	8.1E+01
51	81	0.844	1.04E-02	1.04E-02	8.1E+01
42	87	1.077	1.24E-02	1.24E-02	8.7E+01
49	87	1.077	1.24E-02	1.24E-02	8.7E+01
17	135	2.480	1.84E-02	2.76E-02	9.0E+01
26	135	2.480	1.84E-02	2.76E-02	9.0E+01
52	135	1.782	1.32E-02	1.98E-02	9.0E+01
45	138	1.802	1.31E-02	1.96E-02	9.2E+01
38	276	70.123	2.54E-01	7.62E-01	9.2E+01
36	299	70.846	2.37E-01	7.11E-01	1.0E+02
39	480	71.304	1.49E-01	4.46E-01	1.6E+02
46	480	71.304	1.49E-01	4.46E-01	1.6E+02
9	646	241.084	3.73E-01	2.24E+00	1.1E+02
15	646	247.561	3.83E-01	2.30E+00	1.1E+02
19	646	247.561	3.83E-01	2.30E+00	1.1E+02
23	646	241.084	3.73E-01	2.24E+00	1.1E+02
10	714	203.654	2.85E-01	1.71E+00	1.2E+02
14	714	199.722	2.80E-01	1.68E+00	1.2E+02
18	714	199.722	2.80E-01	1.68E+00	1.2E+02
24	714	203.654	2.85E-01	1.71E+00	1.2E+02
5	800	141.790	1.77E-01	1.06E+00	1.3E+02
27	800	141.790	1.77E-01	1.06E+00	1.3E+02
1	864	169.338	1.96E-01	1.18E+00	1.4E+02
31	864	169.338	1.96E-01	1.18E+00	1.4E+02
35	2646	410.421	1.55E-01	1.86E+00	2.2E+02
37	2646	410.421	1.55E-01	1.86E+00	2.2E+02
40	2816	381.491	1.35E-01	1.63E+00	2.3E+02
47	2816	381.491	1.35E-01	1.63E+00	2.3E+02
4	5529	182.329	3.30E-02	7.91E-01	2.3E+02
8	5529	149.833	2.71E-02	6.50E-01	2.3E+02
30	5529	149.833	2.71E-02	6.50E-01	2.3E+02
34	5529	182.329	3.30E-02	7.91E-01	2.3E+02

4.3 Individual patch mesh adjusting

The patch-tree of each patch is constructed based on the original mesh of Body the body armour in the data structure right after importation. However, the first step of mesh adjusting process does not involve Patch-tree utilization. Due to the huge amount of elements on the original mesh of the body armour, directly applying the Multi-patch adjusting process (3.5.3) will be very time-consuming. Consequently, the process of single-patch undersize elements elimination (Section 3.4.2) is applied to each patch individually with its own lower bound determined before. After all the 52 patches have gone through such a process, an intermediate adjusted mesh of the model is obtained. The updated mesh of the body armour is shown in Figures 4.4 and 4.5. While the updated mesh obtained here does not ensure a perfect fit along the contact boundaries; an example of the mismatching condition is shown in a zoom in perspective of a trouser of the suit in Figure 4.6. The patches information summary of updated mesh is shown in Table 4.4.

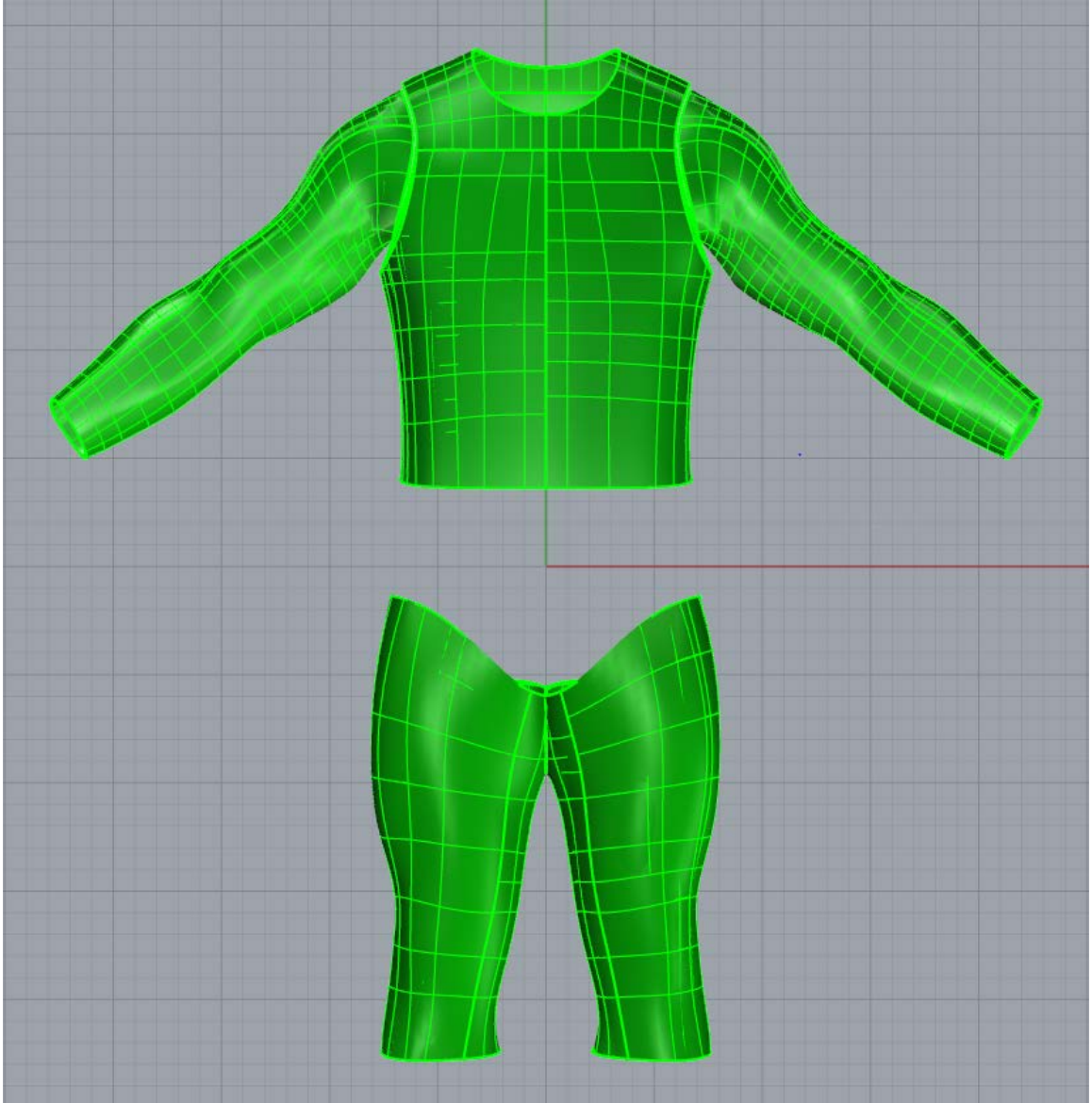


Figure 4.4: Front vision of updated mesh of body armour with undersize elements eliminated

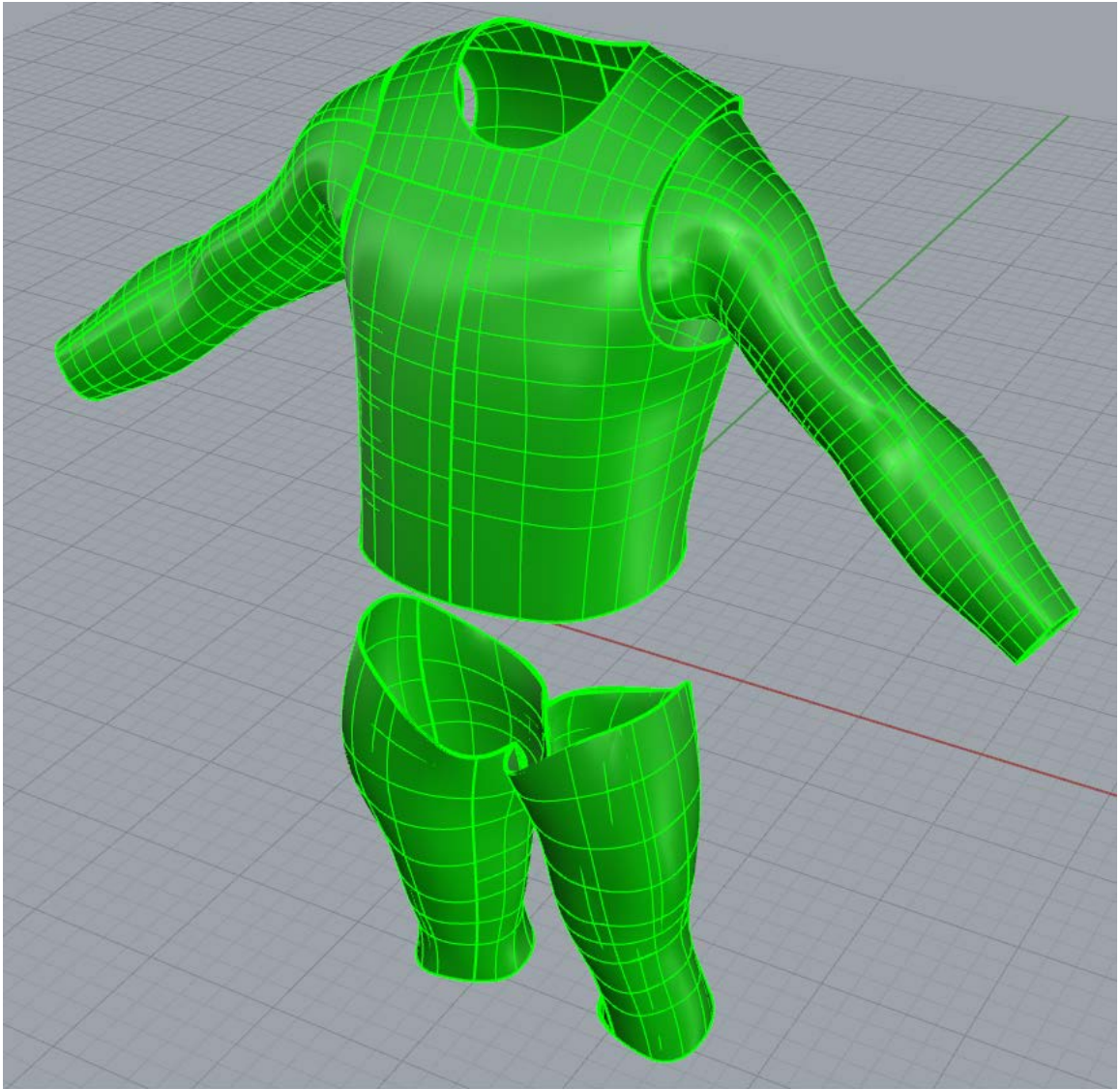


Figure 4.5: Perspective vision of updated mesh of body armour with undersize elements eliminated

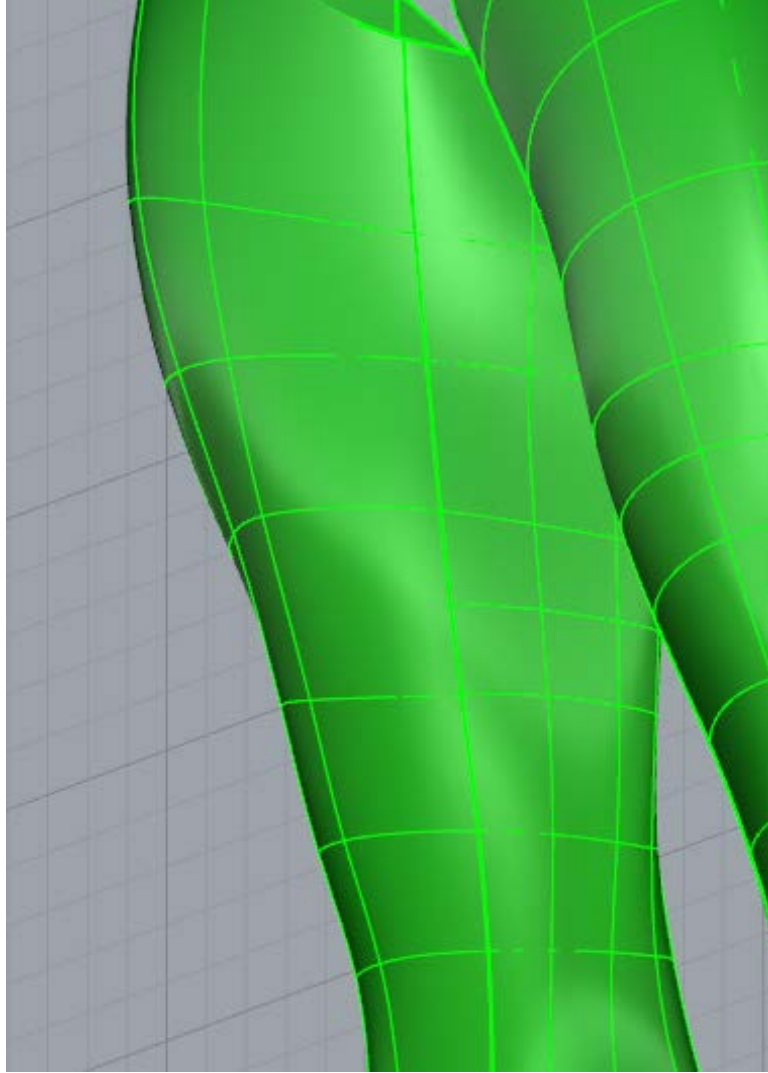


Figure 4.6: Trouser zoom in of updated mesh of body armour with undersize elements eliminated

Table 4.4 Summary of patches information on updated mesh of body armour with undersize elements eliminated

Patch Number	Elements	Patch Area	Element Mean Area
1	76	166.520	2.19E+00
2	30	0.482	1.61E-02
3	33	1.209	3.66E-02
4	150	183.941	1.23E+00
5	85	144.559	1.70E+00
6	28	0.487	1.74E-02
7	28	1.221	4.36E-02
8	144	151.363	1.05E+00
9	45	239.858	5.33E+00
10	56	205.777	3.67E+00
11	43	0.912	2.12E-02
12	6	0.220	3.66E-02
13	68	2.451	3.61E-02
14	36	197.524	5.49E+00
15	42	244.394	5.82E+00
16	41	0.846	2.06E-02
17	45	2.480	5.51E-02
18	56	201.397	3.60E+00
19	45	246.944	5.49E+00
20	41	0.846	2.06E-02
21	6	0.220	3.66E-02
22	68	2.451	3.61E-02
23	48	238.145	4.96E+00
24	36	202.209	5.62E+00
25	43	0.912	2.12E-02
26	45	2.480	5.51E-02
27	95	141.987	1.49E+00
28	28	0.487	1.74E-02
29	28	1.221	4.36E-02
30	108	150.546	1.39E+00
31	76	165.648	2.18E+00
32	30	0.482	1.61E-02
33	33	1.209	3.66E-02
34	132	181.559	1.38E+00
35	99	408.903	4.13E+00
36	56	70.898	1.27E+00
37	105	414.509	3.95E+00
38	49	69.977	1.43E+00
39	84	70.885	8.44E-01

Table 4.4-continued

40	84	380.592	4.53E+00
41	21	0.767	3.65E-02
42	29	1.077	3.71E-02
43	50	1.008	2.02E-02
44	27	0.844	3.13E-02
45	46	1.802	3.92E-02
46	96	70.897	7.39E-01
47	110	375.883	3.42E+00
48	21	0.767	3.65E-02
49	29	1.077	3.71E-02
50	50	1.008	2.02E-02
51	27	0.844	3.13E-02
52	45	1.782	3.96E-02

4.4 Knots Synchronization

After each undersize element elimination step, the elements number of each patch in the model is reduced to an acceptable level. At this point, we can utilize the constructed patch-tree and treat the current adjusted body armour model as a raw designed Multi-patch model (3.6). The knots synchronization process is then applied on the current body armour model (3.6.2), and in fact, to contact patches only. The updated mesh of the body armour model is shown in Figures 4.7 and 4.8; a zoom in perspective of a suit trouser part is shown in Figure 4.9.

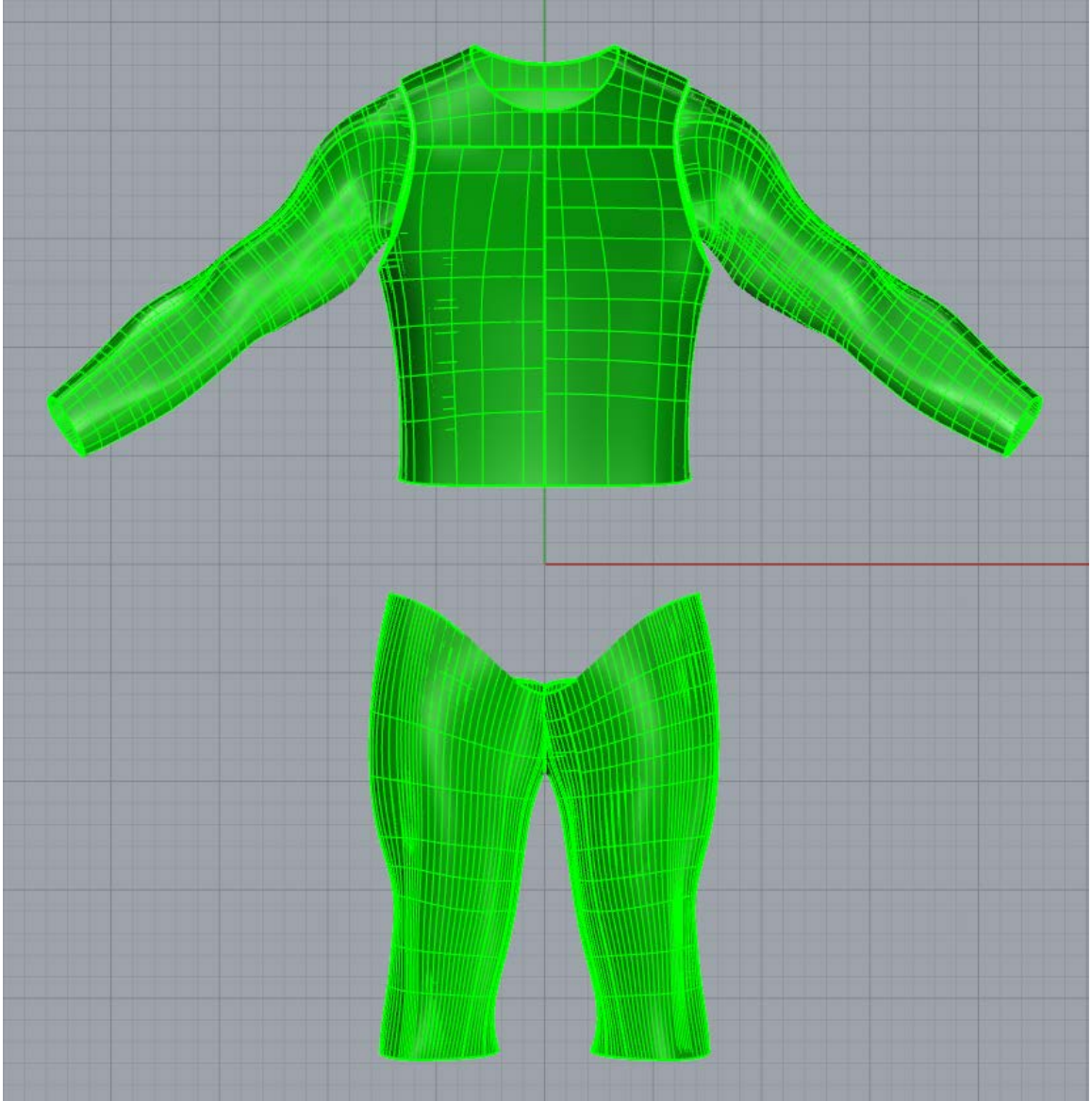


Figure 4.7: Front vision of updated mesh of body armour with knots synchronized

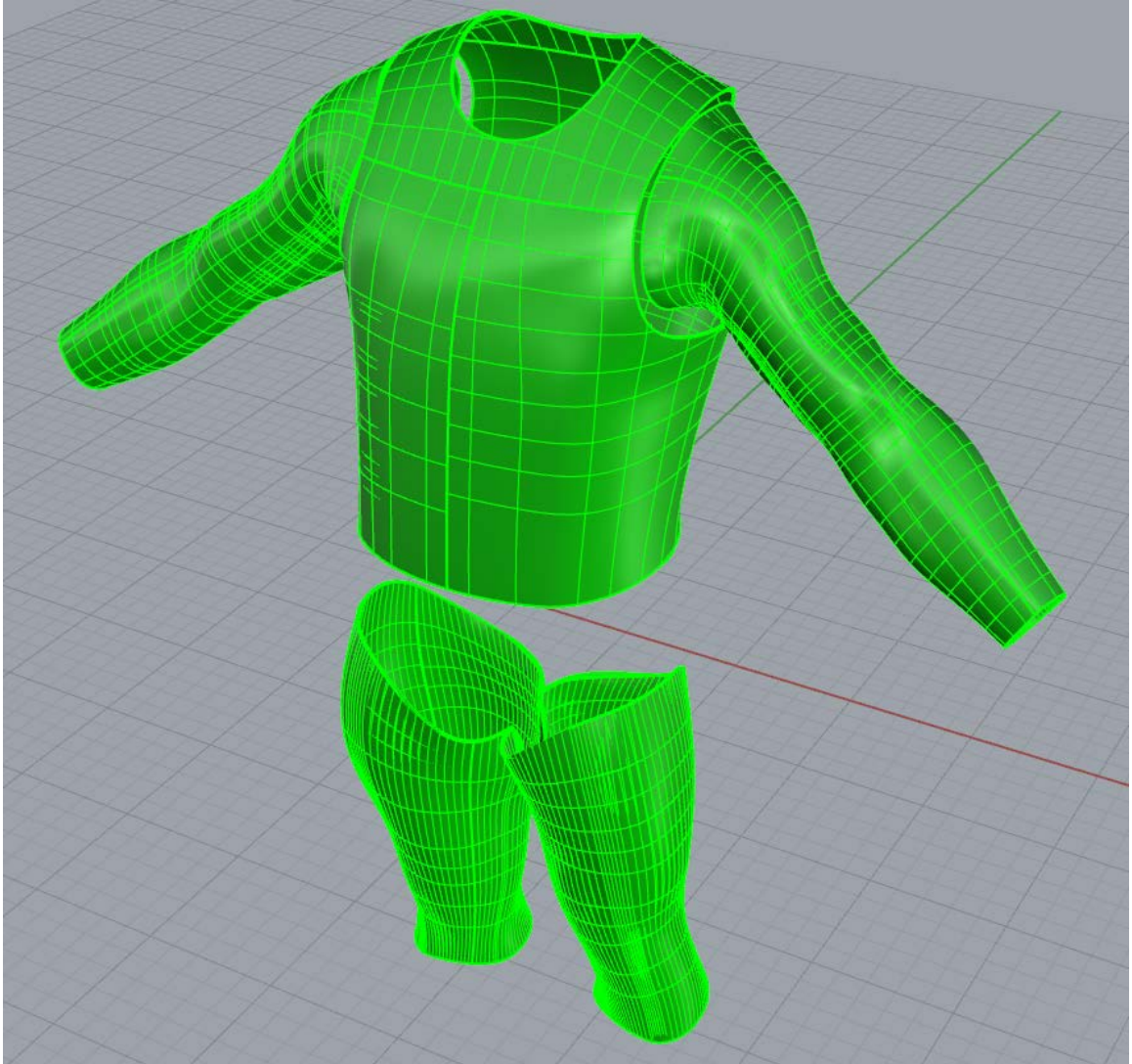


Figure 4.8: Perspective vision of updated mesh of body armour with knots synchronized

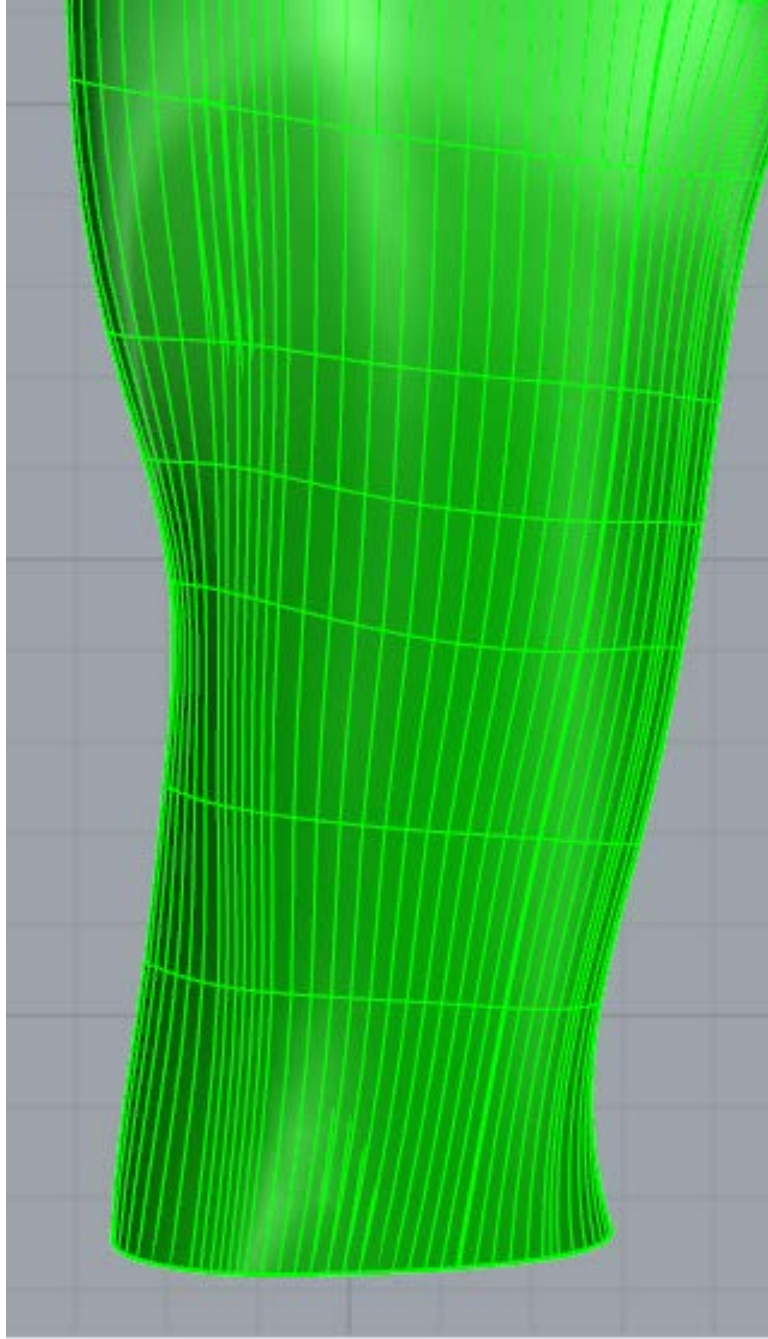


Figure 4.9: Trouser part zoom in of updated mesh of body armour with knots synchronized

4.5 Multi-patch mesh adjusting

4.5.1 Elements breaking

As the knots over contact patches have been synchronized, we utilize patch-tree to apply multi-patch elements elimination process to current model. As we can see from Figures 4.7 and 4.8, due to the knots synchronization process, the updated mesh of some contact patches become too dense again. It is mainly reflected as the imbalance ratio of elements edge lengths in the two directions. Such condition is clearly shown in Figure 4.9. Nevertheless, the mesh of other patches which do not have any contact patch have relatively reasonable distributed elements. In consideration of such situation, the checking index (Section 3.4.2) in the process of element elimination is adjusted for this case. During the searching, if an element has an element edge length ratio over 3 or under $1/3$, knot removal is then applied on the corresponding knot vector to rebuild the element. Other than this, the element elimination procedure remains the same as described in Sections 3.4.2 and 3.5.3. The updated mesh of body armour is shown in Figures 4.10 and 4.11. The patches information of the updated mesh is shown in Table 4.5.

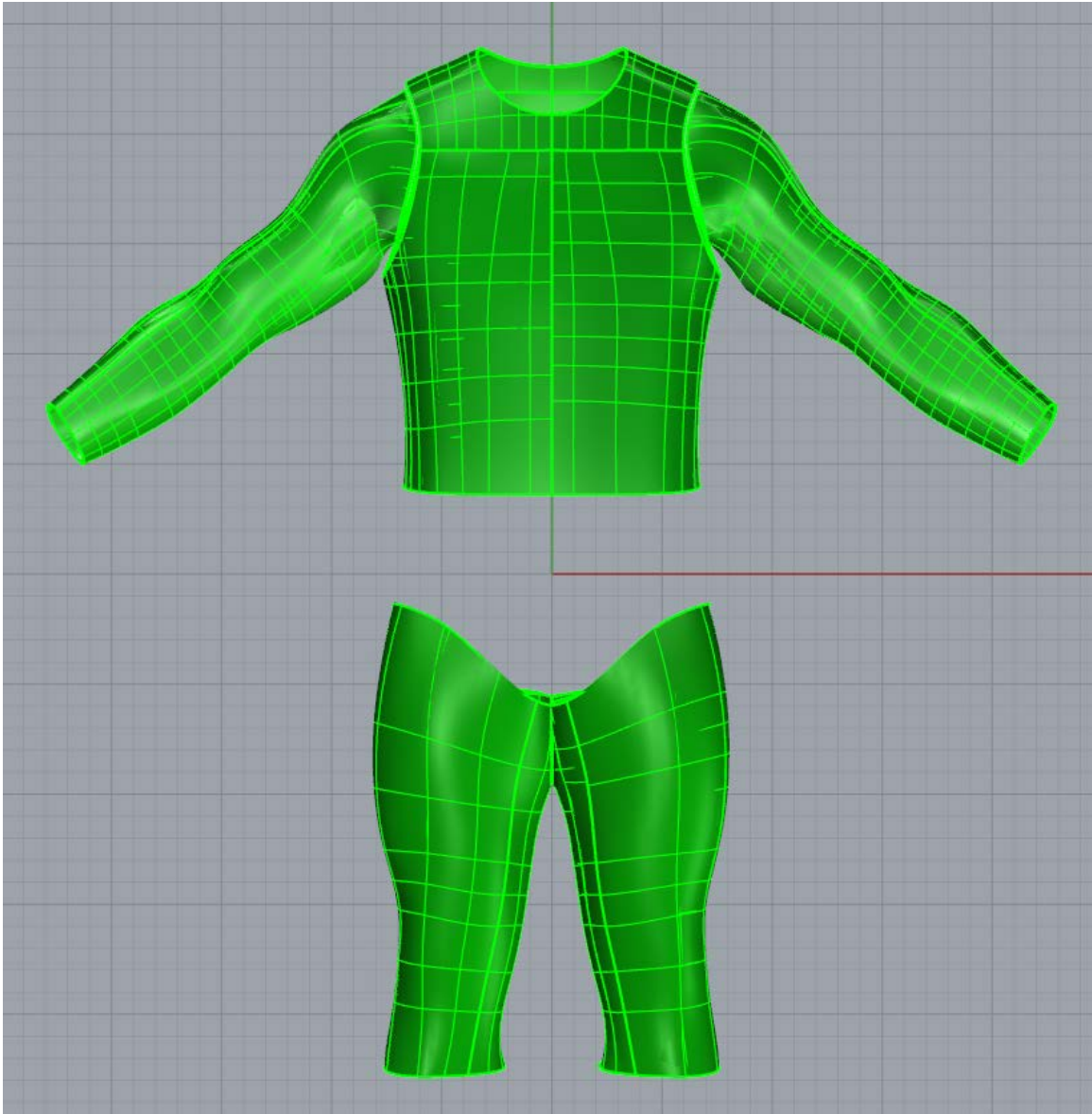


Figure 4.10: Front vision of updated mesh of body armour after imbalanced elements adjusted

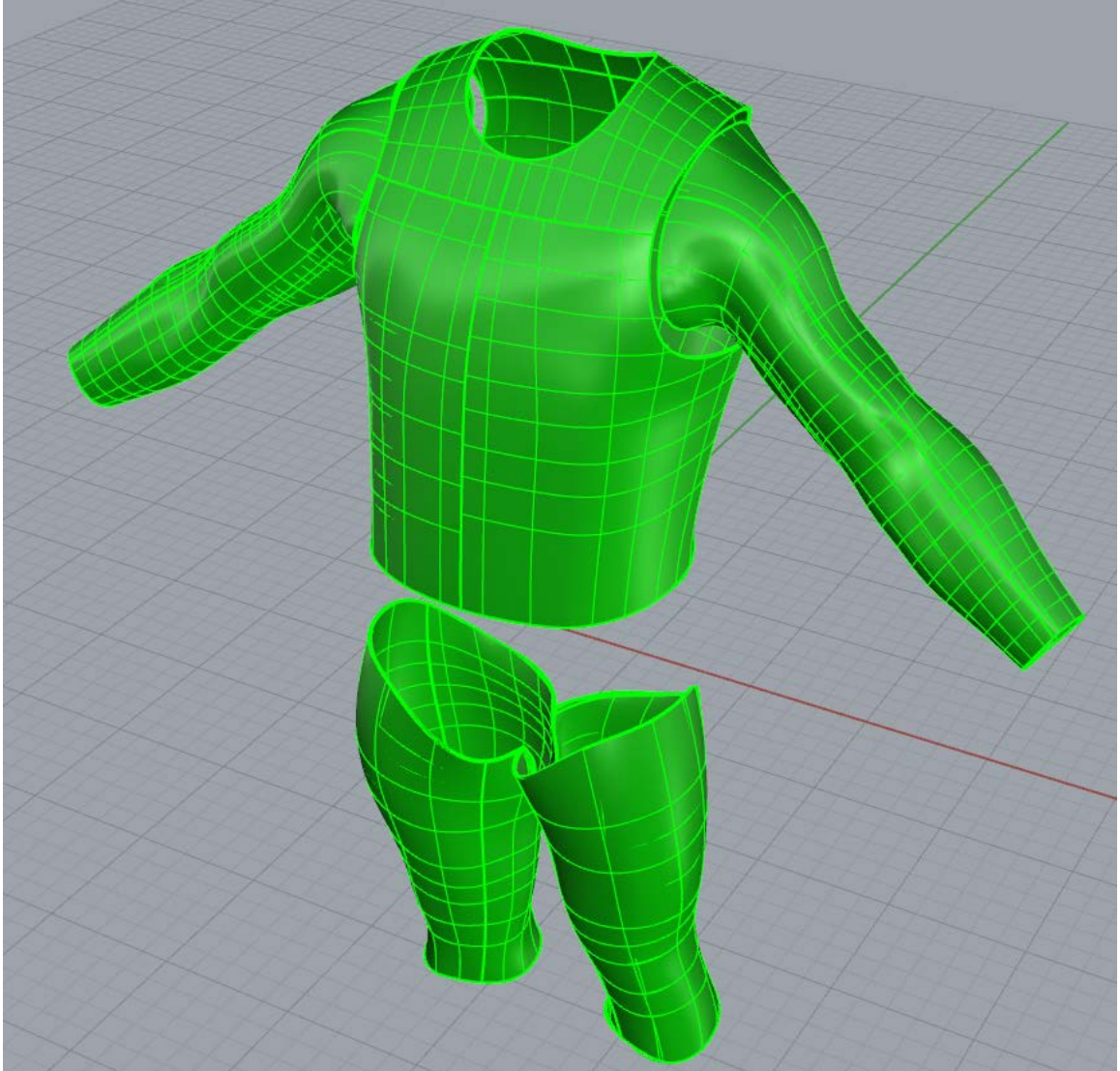


Figure 4.11: Perspective vision of updated mesh of body armour after imbalanced elements adjusted

Table 4.5 Summary of patches information of the updated mesh of body armour after imbalanced elements adjustment

Patch Number	Elements	Patch Area	Element Mean Area
1	162	165.888	1.02E+00
2	29	0.482	1.66E-02
3	8	1.094	1.37E-01
4	108	184.277	1.71E+00
5	144	142.369	9.89E-01
6	28	0.487	1.74E-02
7	9	1.238	1.38E-01
8	108	151.371	1.40E+00
9	66	240.746	3.65E+00
10	64	205.967	3.22E+00
11	8	0.915	1.14E-01
12	6	0.220	3.66E-02
13	68	2.451	3.61E-02
14	88	197.510	2.24E+00
15	48	244.077	5.08E+00
16	6	0.766	1.28E-01
17	45	2.480	5.51E-02
18	56	202.077	3.61E+00
19	40	247.680	6.19E+00
20	5	0.812	1.62E-01
21	6	0.220	3.66E-02
22	68	2.451	3.61E-02
23	40	237.164	5.93E+00
24	56	202.861	3.62E+00
25	7	0.934	1.33E-01
26	45	2.480	5.51E-02
27	176	142.216	8.08E-01
28	28	0.487	1.74E-02
29	11	1.219	1.11E-01
30	90	148.054	1.65E+00
31	242	165.307	6.83E-01
32	29	0.482	1.66E-02
33	8	1.012	1.27E-01
34	60	175.705	2.93E+00
35	99	408.903	4.13E+00
36	56	70.898	1.27E+00
37	84	406.582	4.84E+00
38	49	69.977	1.43E+00
39	35	69.749	1.99E+00

Table 4.5-continued

40	140	379.973	2.71E+00
41	21	0.767	3.65E-02
42	29	1.077	3.71E-02
43	25	1.008	4.03E-02
44	27	0.844	3.13E-02
45	46	1.802	3.92E-02
46	42	69.773	1.66E+00
47	110	375.307	3.41E+00
48	21	0.767	3.65E-02
49	29	1.077	3.71E-02
50	25	1.008	4.03E-02
51	27	0.844	3.13E-02
52	45	1.782	3.96E-02

4.5.2 Elements refinement

After the application of the element elimination process performed in Section 4.5.1, the body armour has a relatively sparse mesh. In order to improve the mesh condition, the overall mesh of the current model needs slight refinement. A process of elements refinement is then applied to the model. The process follows the procedure of oversize element refinement in Multi-patch adjusting (Section 3.5.3). The upper bound is set as two times of the current element area mean for each patch. The refinement process re-calculates the control points and other control parameters (Section 3.5.4). After this step, the whole process of mesh adjusting for the body armour is completed. A new IGES file with the updated body armour is then generated via IGES Writer. The final updated mesh of the body armour is shown in Figures 4.12 and 4.13. Figures 4.14-4.16 show the zoom in perspectives on final updated mesh of the body armour of the same regions shown in Figure 4.3, 4.6 and 4.9 respectively. The patches information summary of the final updated body armour model is summarized in Table 4.6.

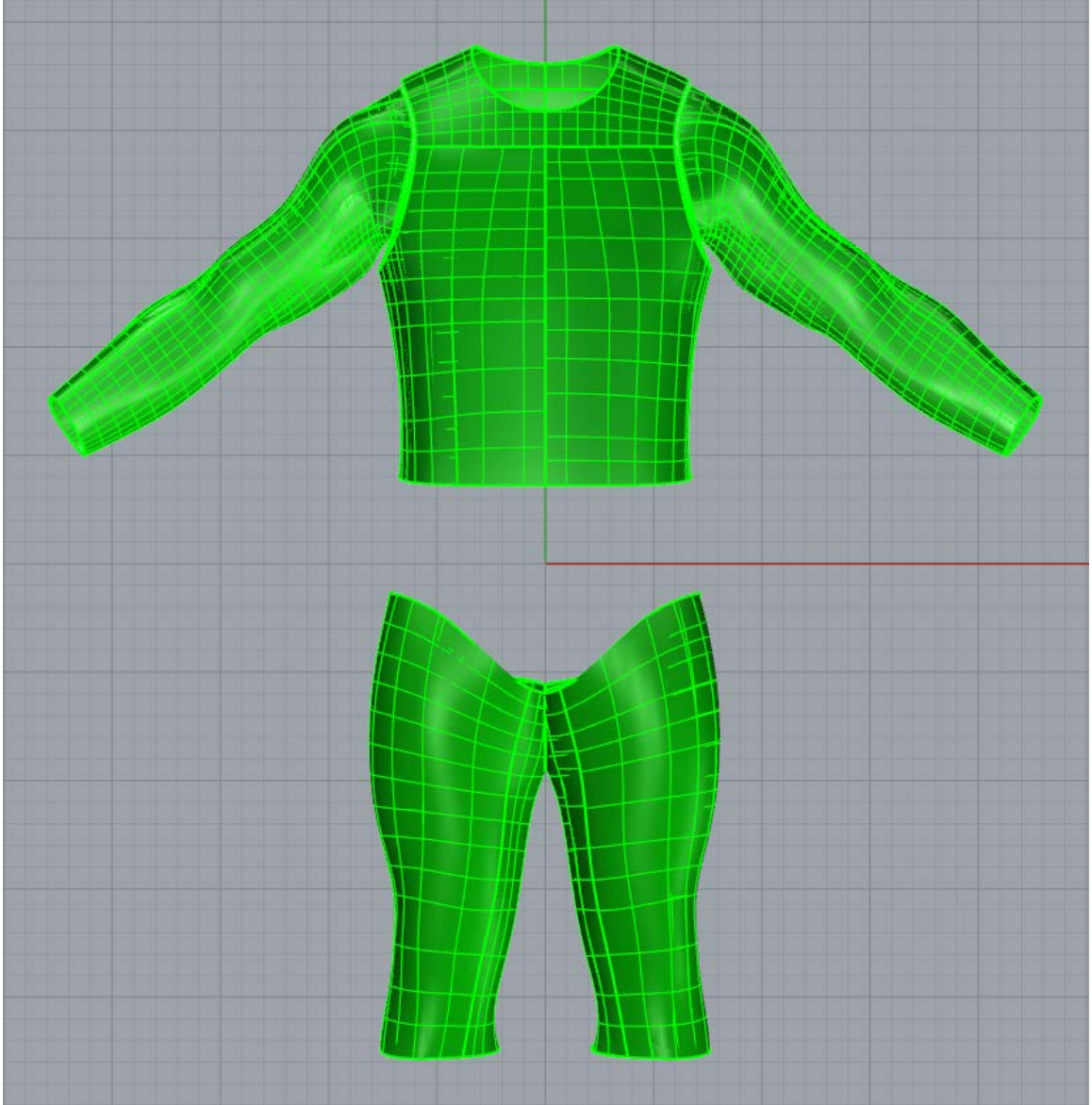


Figure 4.12: Front vision of final updated mesh of body armour

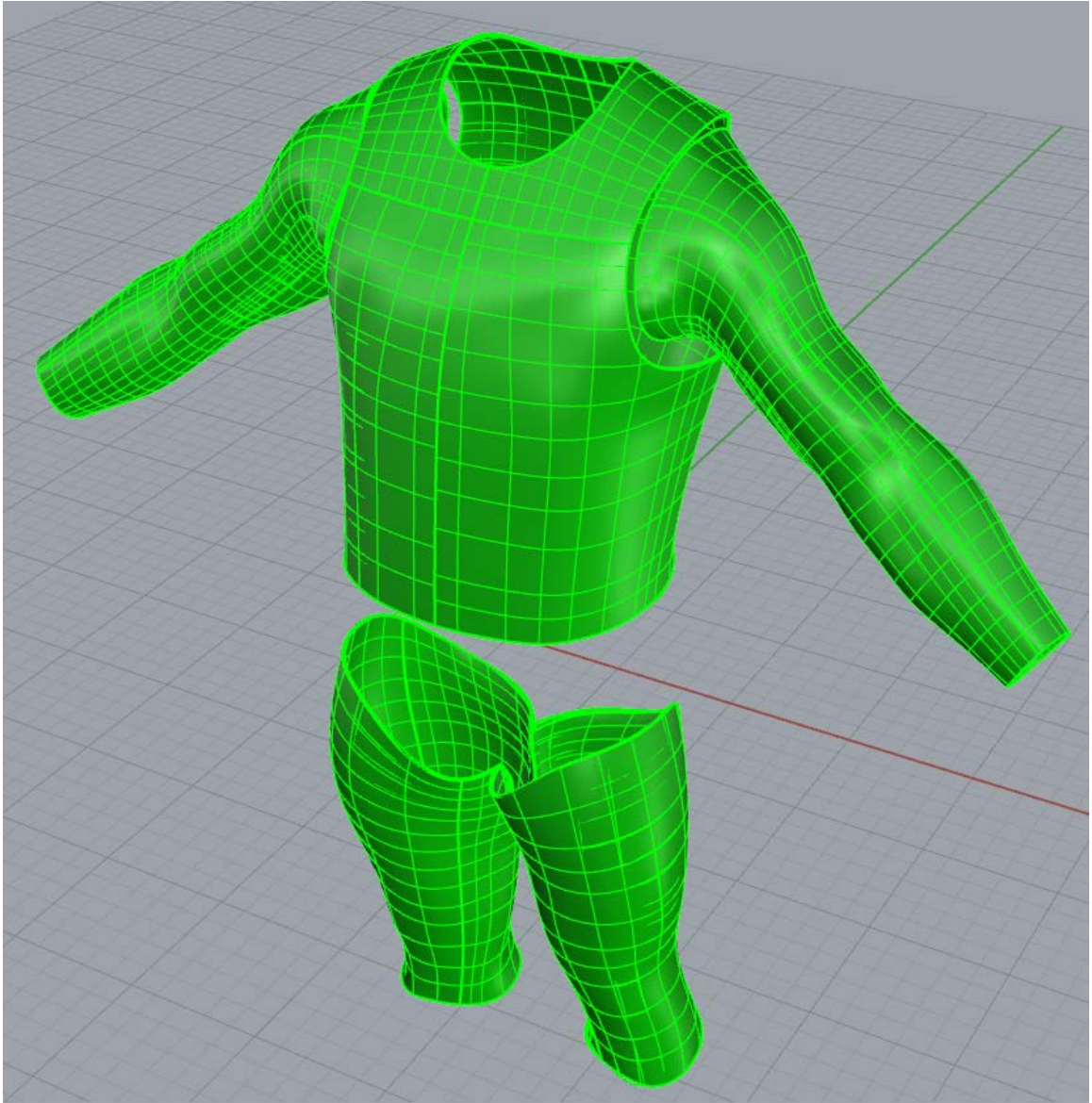


Figure 4.13: Perspective vision of final updated mesh of body armour

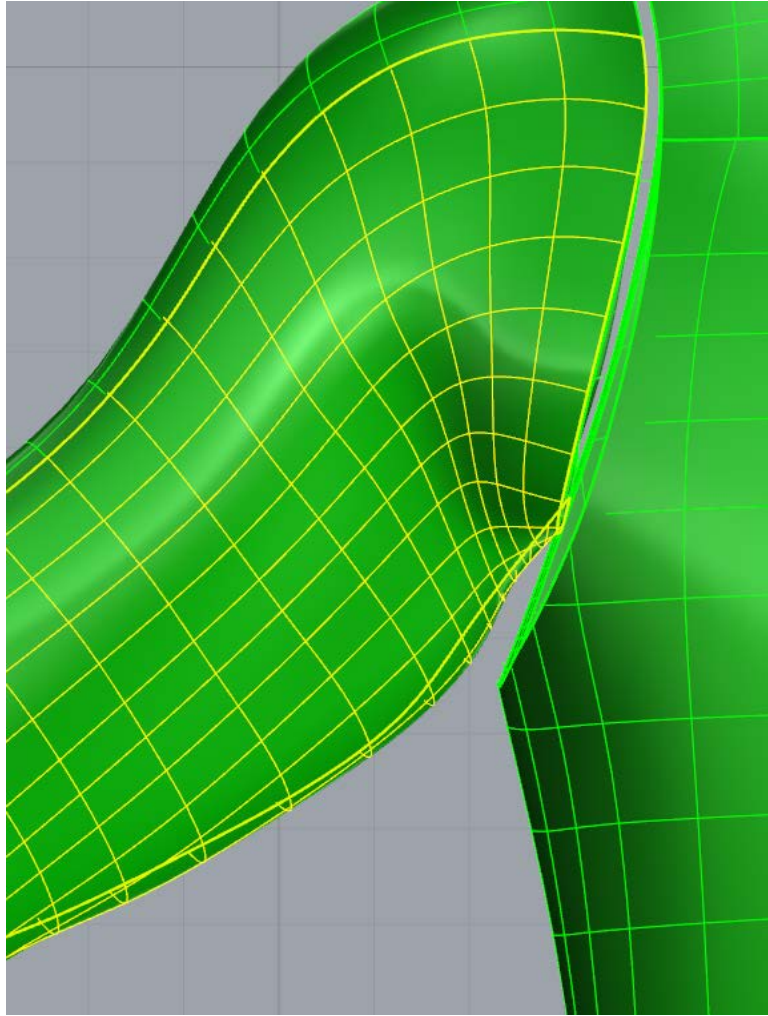


Figure 4.14: Sleeve zoom in of final updated mesh of body armour

Compared with the mesh condition shown in Figure 4.3, it is clear that the overly dense condition of the original model is significantly improved.

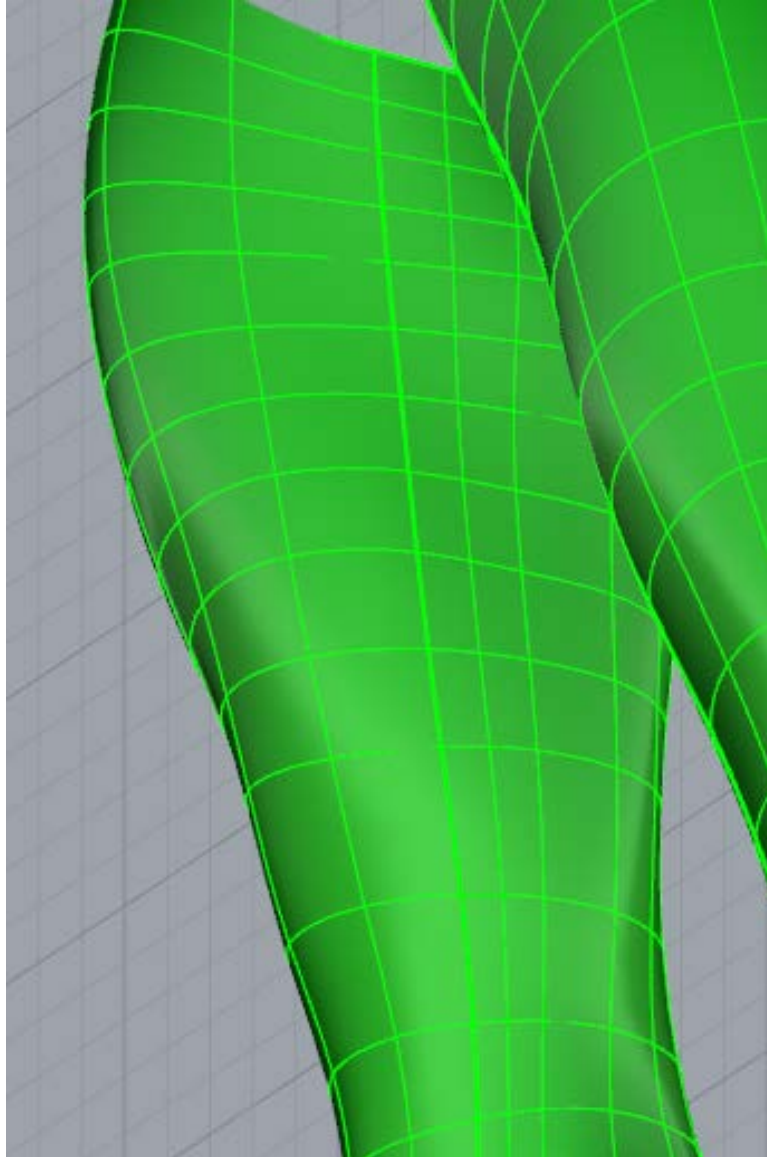


Figure 4.15: Trouser zoom in of final updated mesh of body armour

The mismatching condition (Figure 4.6) caused by the element breaking process in section 4.3 has been fixed. The final updated model maintains the uniformity of the mesh across presumably contact patch boundaries in the original Body armour model.

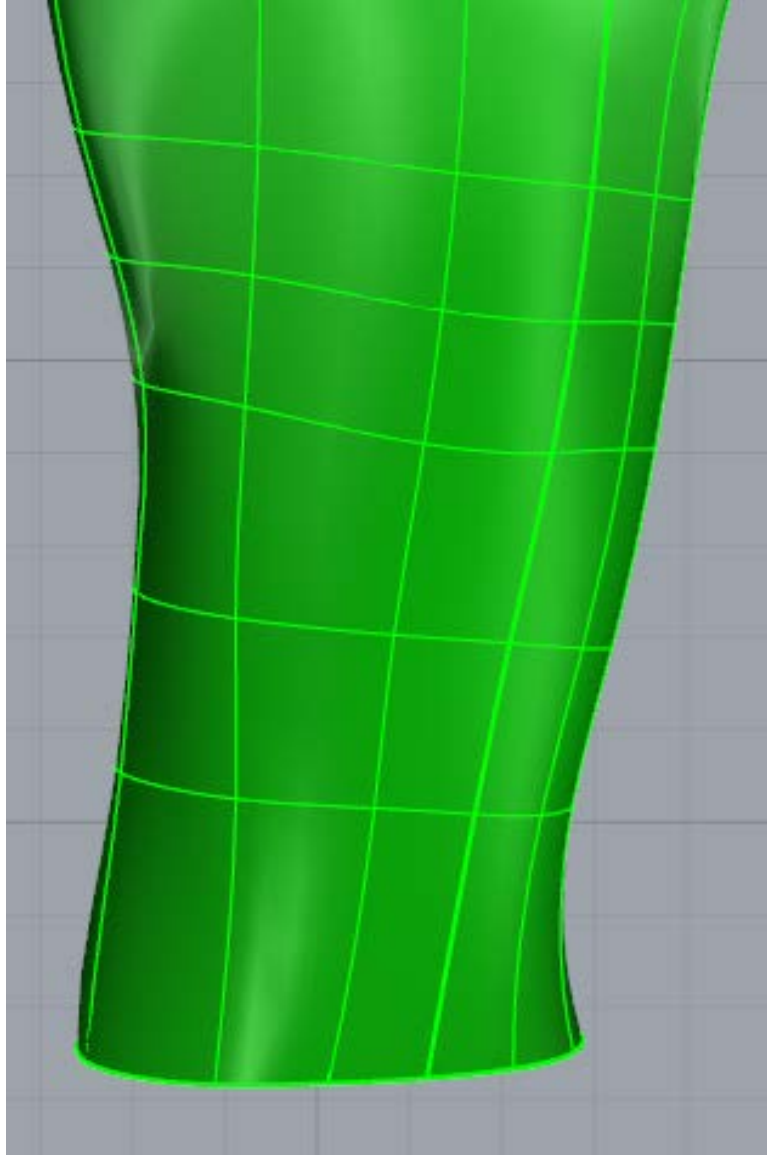


Figure 4.16: Trouser part zoom in of final updated mesh of body armour

Through a comparison with the mesh shown in Figure 4.9, the condition of imbalanced ratio of elements edge lengths in the two directions has been improved.

Table 4.6 Summary of patches information on final updated mesh of body armour

Patch Number	Elements	Patch Area	Element Mean Area
1	464	165.888	3.58E-01
2	43	0.482	1.12E-02
3	15	1.094	7.29E-02
4	264	184.277	6.98E-01
5	435	142.369	3.27E-01
6	41	0.487	1.19E-02
7	16	0.748	4.68E-02
8	240	151.371	6.31E-01
9	135	240.746	1.78E+00
10	168	205.967	1.23E+00
11	12	0.919	7.66E-02
12	11	0.220	2.00E-02
13	101	2.451	2.43E-02
14	180	197.510	1.10E+00
15	126	244.078	1.94E+00
16	9	0.534	5.93E-02
17	90	2.480	2.76E-02
18	126	202.077	1.60E+00
19	84	247.680	2.95E+00
20	7	0.865	1.24E-01
21	11	0.220	2.00E-02
22	101	2.451	2.43E-02
23	98	237.167	2.42E+00
24	108	202.861	1.88E+00
25	9	0.620	6.89E-02
26	90	2.480	2.76E-02
27	525	142.216	2.71E-01
28	41	0.487	1.19E-02
29	16	1.219	7.62E-02
30	288	148.054	5.14E-01
31	560	165.307	2.95E-01
32	43	0.482	1.12E-02
33	15	1.920	1.28E-01
34	168	175.634	1.05E+00
35	216	408.903	1.89E+00
36	104	70.898	6.82E-01
37	180	406.582	2.26E+00
38	96	69.977	7.29E-01
39	77	69.749	9.06E-01
40	270	379.973	1.41E+00

41	30	0.767	2.56E-02
42	40	1.077	2.69E-02
43	37	1.008	2.73E-02
44	40	0.844	2.11E-02
45	91	1.802	1.98E-02
46	88	69.773	7.93E-01
47	225	375.307	1.67E+00
48	30	0.767	2.56E-02
49	40	1.077	2.69E-02
50	37	1.008	2.73E-02
51	40	0.844	2.11E-02
52	77	1.782	2.31E-02

4.6 Conclusions

The overly dense mesh of the original body armour model is automatically modified. The total number of elements in the model is reduced from 45054 to 6358. The largest element number in a patch of adjusted model is 560. The overly dense patches which have over 2000 elements in original model are all adjusted to around 10% of the original number. For the contact patches in original model, the contact boundaries have matching control parameters ensuing a perfect fit along the boundary.

CHAPTER 5 CONCLUSIONS

An IGA preprocessor is developed in this study for converting a raw CAD model to an ASG model. The preprocessor specifically deals with the CAD model which is created with NURBS surfaces and stored as an IGES format. The preprocessor is able to automatically adjust the CAD model's initial mesh based on the requirement of users. The utilization of the knot insertion algorithm and the knot removal algorithm in the preprocessor makes it possible to control the overall elements size and the element edge ratio in the two directions. The multi-patch tree technology is able to maintain and enhance the uniformity of the mesh across presumably contact boundaries in Multi-patch NURBS model. This satisfies the requirement for the geometric continuity over boundaries in IGA. Through utilizing the pre-processor to deal with a raw CAD model in real world, it has been demonstrated that all major goals of the study have been reached.

The major limitation of the current IGA preprocessor is related to trimmed boundary. In real world a lot of CAD models are designed by using trimmed NURBS [19]. Some of the NURBS patches are contacted along a trimmed boundary other than common patch boundary. The trimmed boundary curves have a sort of geometric representation which is totally different than NURBS [19]. When dealing with a CAD model that contains trimmed boundaries, the current IGA preprocessor cannot ensure geometric continuity over boundaries after this process. This issue can be investigated in future study. With the further research on the trimmed curve geometry, it can be expected that the function to deal with the trimmed boundaries can be successfully included in our IGA preprocessor.

REFERENCES

1. Hughes, T.J.R., J.A. Cottrell, and Y. Bazilevs, *Isogeometric analysis: CAD, finite elements, NURBS, exact geometry and mesh refinement*. Computer Methods in Applied Mechanics and Engineering, 2005. **194**(39–41): p. 4135-4195.
2. Chen, J.S., et al., *Some recent improvements in meshfree methods for incompressible finite elasticity boundary value problems with contact*. Computational Mechanics, 2000. **25**(2-3): p. 137-156.
3. Piegl, L. and W. Tiller, *The NURBS Book*. 1995, Berlin: Springer.
4. Cottrell, J.A., T.J.R. Hughes, and Y. Bazilevs, *Isogeometric Analysis: Toward Integration of CAD and FEA*. 2009, Chichester: John Wiley & Sons, Ltd.
5. Bazilevs, Y., et al., *Isogeometric analysis using T-splines*. Computer Methods in Applied Mechanics and Engineering, 2010. **199**(5–8): p. 229-263.
6. Cottrell, J.A., T.J.R. Hughes, and A. Reali, *Studies of refinement and continuity in isogeometric structural analysis*. Computer Methods in Applied Mechanics and Engineering, 2007. **196**(41–44): p. 4160-4183.
7. Cohen, E., et al., *Analysis-aware modeling: Understanding quality considerations in modeling for isogeometric analysis*. Computer Methods in Applied Mechanics and Engineering, 2010. **199**(5–8): p. 334-356.
8. Xu, G., et al., *Analysis-suitable volume parameterization of multi-block computational domain in isogeometric applications*. Computer-Aided Design, 2013. **45**(2): p. 395-404.
9. Nguyen, V., et al., *Nitsche's method for two and three dimensional NURBS patch coupling*. Computational Mechanics, 2014. **53**(6): p. 1163-1182.
10. Takacs, T. and B. Jüttler, *Existence of stiffness matrix integrals for singularly parameterized domains in isogeometric analysis*. Computer Methods in Applied Mechanics and Engineering, 2011. **200**(49–52): p. 3568-3582.

11. Xu, G., et al., *Parameterization of computational domain in isogeometric analysis: Methods and comparison*. Computer Methods in Applied Mechanics and Engineering, 2011. **200**(23–24): p. 2021-2031.
12. Schmidt, R., et al., *Realization of an integrated structural design process: analysis-suitable geometric modelling and isogeometric analysis*. Computing and Visualization in Science, 2010. **13**(7): p. 315-330.
13. Lu, J., *Circular element: Isogeometric elements of smooth boundary*. Computer Methods in Applied Mechanics and Engineering, 2009. **198**(30–32): p. 2391-2402.
14. Lu, J. and C. Zheng, *Dynamic cloth simulation by isogeometric analysis*. Computer Methods in Applied Mechanics and Engineering, 2014. **268**: p. 475-493.
15. Kiendl, J., et al., *Isogeometric shell analysis with Kirchhoff–Love elements*. Computer Methods in Applied Mechanics and Engineering, 2009. **198**(49–52): p. 3902-3914.
16. Rogers, D.F., *An Introduction to NURBS: With Historical Perspective*. 2001, San Diego: Morgan Kaufmann Publishers.
17. Lu, J., *Isogeometric contact analysis: Geometric basis and formulation for frictionless contact*. Computer Methods in Applied Mechanics and Engineering, 2011. **200**(5–8): p. 726-741.
18. Lu, J. and X. Zhou, *Cylindrical element: Isogeometric model of continuum rod*. Computer Methods in Applied Mechanics and Engineering, 2011. **200**(1–4): p. 233-241.
19. Kim, H.-J., Y.-D. Seo, and S.-K. Youn, *Isogeometric analysis for trimmed CAD surfaces*. Computer Methods in Applied Mechanics and Engineering, 2009. **198**(37–40): p. 2982-2995.
20. Bazilevs, Y., et al., *Isogeometric analysis: Approximation, stability and error estimates for h-refined meshes*. Mathematical Models and Methods in Applied Sciences, 2006. **16**(7): p. 1031-1090.

21. Cottrell, J.A., et al., *Isogeometric analysis of structural vibrations*. Computer Methods in Applied Mechanics and Engineering, 2006. **195**(41–43): p. 5257-5296.
22. Keckeisen, M., et al. *Interactive cloth simulation in virtual environments*. in *Virtual Reality, 2003. Proceedings. IEEE*. 2003.
23. Liu, Y.-J., D.-L. Zhang, and M.M.-F. Yuen, *A survey on CAD methods in 3D garment design*. Computers in Industry, 2010. **61**(6): p. 576-593.
24. *Gerber in United States*. Available from: <http://www.gerbertechnology.com/>.
25. *Investronica in Spain*. Available from: <http://www.investronica-sis.es/>.
26. *Lectra in France*. Available from: <http://www.lectra.com/en/index.html>.
27. *Assyst-Bullmer in German*. Available from: <http://www.assyst-intl.com/>.
28. *Dessingsim in Japan*. Available from: <http://www.dressingsim.com/>.
29. Simo, J.C. and D.D. Fox, *On a stress resultant geometrically exact shell model. Part I: Formulation and optimal parametrization*. Computer Methods in Applied Mechanics and Engineering, 1989. **72**(3): p. 267-304.
30. Simo, J.C., D.D. Fox, and M.S. Rifai, *On a stress resultant geometrically exact shell model. Part II: The linear theory; Computational aspects*. Computer Methods in Applied Mechanics and Engineering, 1989. **73**(1): p. 53-92.
31. Volino, P., F. Cordier, and N. Magnenat-Thalmann, *From early virtual garment simulation to interactive fashion design*. Computer-Aided Design, 2005. **37**(6): p. 593-608.